npj | flexible electronics

Review

Published in partnership with Nanjing Tech University

https://doi.org/10.1038/s41528-026-00537-5

4A tetrahedron system: a synergistic framework for panvascular intervention empowered by flexible electronics

Check for updates

Lingsen You[1,2,3,4,5,7], Yirong Qu[1,2,4,5,7], Yuheng Chen[1,2,4,5,7], Yu Wang[6,7], Li Shen[1,2,3,4,5] ✉ & Junbo Ge[1,2,3,4,5] ✉

This review introduces the "4 A Tetrahedron System" (Assessment, Assistance, Aftercare, AI-retrofit) as a synergistic framework for panvascular intervention empowered by flexible electronics. Central to this is the novel concept of "suitcordance"—short-term suitability and long-term concordance. By integrating flexible sensors, navigation tools, and AI algorithms, this framework establishes a closed-loop data ecosystem, driving a transition toward intelligent, full-cycle disease management.

Panvascular disease, characterized by the common pathological feature of atherosclerosis (which accounts for 95% of cases), is a group of systemic vascular disorders affecting vital organs such as the heart, brain, kidneys, and limbs. In its broader definition, it also encompasses diseases of small and micro-vessels, veins, and vascular conditions related to diabetes and immunity, collectively representing the "number one killer" of human health[1]. According to the Global Burden of Disease (GBD) database, the incidence, prevalence, and mortality of panvascular disease are increasing annually. Notably, in 2021, the Disability-Adjusted Life Year (DALY) metric for cardiovascular diseases alone reached 428 million[2], painting a grim picture. Panvascular disease has thus become a significant threat to human life and global public health security.

Interventional therapy has emerged as a crucial strategy for addressing the challenges of panvascular disease[3], owing to its advantages of being minimally invasive, precise, and repeatable, coupled with short recovery times and fewer perioperative complications[4]. However, current interventional treatments still face significant clinical limitations. Conventional passive navigation tools are limited in their ability to precisely target in complex vascular structures, such as the M3 segment of the middle cerebral artery (MCA)[5]. Furthermore, there is often a low degree of "suitcordance"[6]—encompassing both short-term suitability and long-term concordance-between existing interventional devices and blood vessels. Conventional follow-up approaches lack real-time monitoring, thereby failing to effectively mitigate the risk of postoperative recurrence. There is an urgent need to inject cutting-edge innovation to achieve a breakthrough. Fortunately, interventional medicine has recently demonstrated a strong capacity for interdisciplinary exploration. In the future, a deep integration with advanced flexible electronics may open up new and broad prospects for interventional therapy.

This review introduces and systematically explores the concept of "suitcordance", defined as the achievement of short-term suitability (e.g., mechanical and structural compatibility) and long-term concordance (e.g., physiological and biological harmony) between an interventional device and the target vessel. We posit that achieving optimal suitcordance requires a paradigm shift from passive devices to intelligent systems empowered by flexible electronics, which provide the continuous, high-fidelity data necessary for its evaluation and maintenance throughout the therapeutic lifecycle.

Flexible electronics is a novel technology that involves depositing organic/inorganic electronic components onto flexible or ductile substrates to form circuits[7]. Compared to traditional electronic devices, flexible electronics can maintain stable performance while accommodating a certain degree of deformation and adapting to various working environments[8]. The deformability and self-adjustability of innovative material shapes endow flexible electronic devices with wearable and implantable advantages[9–12]. Their stretchability is even compatible with vascular compliance, and their high flexibility meets the requirements of the vascular elastic modulus[13]. Leveraging other excellent properties such as high sensitivity, high accuracy, and integrability[14,15], flexible electronic devices have already achieved notable success in the health monitoring of panvascular diseases affecting the heart, brain, and peripheral vessels[16–18]. With increasing demand, technological advancements, and performance enhancements, the flexible electronics market is exhibiting a strong compound annual growth rate (CAGR), demonstrating its immense market potential and laying a solid foundation for its deep integration with interventional therapy.

The potential of flexible electronics to address the systemic challenges of panvascular disease in full-cycle interventional management currently lacks a systematic theoretical foundation, underscoring the need for an

[1]Department of Cardiology, Zhongshan Hospital, Shanghai Institute of Cardiovascular Diseases, Fudan University, Shanghai, China. [2]National Clinical Research Center for Interventional Medicine, Shanghai, China. [3]University of Shanghai for Science and Technology (USST), Oriental Pan-Vascular Devices Innovation College, Shanghai, China. [4]State Key Laboratory of Cardiovascular Diseases, Zhongshan Hospital, Fudan University, Shanghai, China. [5]NHC Key Laboratory of Ischemic Heart Diseases, Shanghai, China. [6]Department of Cardiology, Shidong Hospital, Shanghai, China. [7]These authors contributed equally: Lingsen You, Yirong Qu, Yuheng Chen, Yu Wang. ✉e-mail: Shen.li1@zs-hospital.sh.cn; jbge@zs-hospital.sh.cn

integrated synergistic framework. Based on this need, we propose the "4 A Tetrahedron System" (Assessment-Assistance-Aftercare-Al-retrofit) to vividly represent the crucial role of flexible electronic devices throughout the entire process of panvascular interventional therapy.

In the Assessment stage, flexible sensing devices are leveraged to establish a synergistic mechanism between preoperative patient profiling and interventional device evaluation. This involves exploring a novel paradigm for interstitial fluid (ISF)-based laboratory examinations and maintaining the homeostatic balance of the three major ecosystems—mechanical, cellular, and physicochemical-immune—at the device-vessel interface, thereby further enhancing "suitcordance". In the Assistance stage, flexible electronic devices will aid intraoperative guidance from both imaging and navigation perspectives, comprehensively enhancing the safety and flexibility of surgical procedures. In the Aftercare stage, flexible health monitoring devices align with the development trend of the "Internet of Medical Things" (IoMT)[19]. They emphasize the real-time nature of postoperative follow-up through multi-dimensional monitoring and remote warning functions, thereby adding momentum to the construction of "Medical Wireless Sensor Networks". Finally, the introduction of AI-retrofit algorithms adds a three-dimensional aspect to the entire framework. By analyzing data collected by flexible electronic devices throughout the patient's interventional journey, consistent patterns can be identified. Real-world clinical cases can inform the continuous optimization of interventional device performance, while data streams foster a virtuous cycle of feedback across the Assessment, Assistance, Aftercare, and AI-based refinement stages.

Flexible electronics will act as an adhesive, connecting the three elements of Assessment, Assistance, and Aftercare to form a triangular "base" plane. This base represents the reinforcement of stability in panvascular interventional therapy from the preoperative, intraoperative, and postoperative dimensions. Artificial intelligence serves as a catalyst, endowing the AI-retrofit stage with the symbolic significance of an "upper vertex" that radiates over the "base". This promotes the framework's transformation from a circular two-dimensional triangle to a dynamic three-dimensional tetrahedron. This framework drives bidirectional and overall circulation along the six edges of the tetrahedron, thereby establishing a complete "4 A Tetrahedron System" comprising four stages, six routes, and twelve relationships.

The "4 A Tetrahedron System" is not merely a synthesized architecture for preoperative diagnosis and assessment, intraoperative assistance, and postoperative monitoring and care in panvascular interventional therapy from the perspective of flexible electronics. It also highlights the pervasive and leading role of artificial intelligence in cutting-edge explorations of medical-engineering integration, establishing a new evaluation standard and development direction for the "full-process" management of panvascular disease.

Assessment: ISF-centered biomarker quantification & interventional device optimization

The preoperative period in panvascular interventional therapy is a critical window for patient examination, monitoring, and the functional pre-setting of devices. With the involvement of flexible sensing devices, the Assessment stage of the "4 A Tetrahedron System" proceeds from two dimensions: the patient and the device. It aims not only to advance point-of-care diagnostics[20] based on interstitial fluid (ISF) to meet laboratory standards for minimally invasive and painless analysis of disease severity, thereby providing accurate guidance for subsequent surgical choices, but also to translate clinical data into improved designs for interventional devices. This involves comprehensively evaluating the harmony of the three ecosystems—mechanical, cellular, and physicochemical-immune—between the device and the vessel, which forms the fundamental basis for quantifying and optimizing device suitcordance, and identifying the optimal path for integrating flexible sensing devices.

The Assessment stage moves beyond the traditional patient-centric paradigm in clinical diagnostics, thereby enabling seamless integration of flexible electronic devices into the preoperative phase of panvascular interventional therapy. By designing and optimizing "smart" interventional devices empowered by flexible electronics in the Assessment stage, the short-term suitability and long-term concordance between the interventional device and the blood vessel will be greatly improved, achieving a long-term shared destiny of the "device and human body".

Redefining laboratory examination paradigms with flexible microneedle platforms

Microneedle arrays applied to the skin surface can penetrate the stratum corneum to reach the dermis without touching nerve endings and blood vessels[21]. They are commonly used for the minimally invasive and painless collection of interstitial fluid (ISF) and to facilitate transdermal drug delivery[22]. Flexible microneedle platforms, which combine flexible substrates with integrated sensing technology, can overcome the barriers of traditional blood analysis, such as long processing times and the need for specialized expertise[23]. They also circumvent the limitations of fingertip or venous blood collection, such as pain and infection risk[23], thereby facilitating rapid and accurate biomarker quantification in ISF samples from patients (Fig. 1a). Compared to other bodily fluids, ISF, which is produced by capillary filtration, has the highest dynamic similarity to blood in terms of composition and biomarker concentrations, making it the most promising alternative to blood for laboratory tests[24]. Excellent flexibility, conformability, and biocompatibility endow the flexible microneedle platform with the capability to guide the monitoring of the three major ecosystem balances: vascular mechanics, cellular, and physicochemical-immune. This lays the foundation for enhancing device suitcordance in subsequent stages and ultimately achieving the goal of a long-term shared destiny between the "device and vessel". In the future, this ISF-based point-of-care diagnostic method is poised to reshape laboratory examination paradigms and become a powerful tool for patients' Assessment in the preoperative stage of panvascular interventional therapy.

Inflammation is a common pathological phenomenon in panvascular disease. Reliable quantification of cytokine levels via flexible microneedle platforms could facilitate preoperative diagnosis in patients with panvascular disease. Xu et al.[25] functionalized microneedle surfaces with antibodies and a carbon nanotube interface to enable selective capture of interleukin-6 (IL-6) from interstitial fluid. Integration with gold microelectrodes yields a sensing module that enables real-time monitoring of cytokine concentrations via in-situ electrical signal modulation, while simplifying the pre-analytical procedures required in conventional laboratory assays, including sample acquisition, preprocessing, and concentration steps. To minimize non-specific protein fouling on the blank regions of the microneedle electrodes, bovine serum albumin (BSA) coating was employed, exhibiting remarkable specificity in both in vitro fluid models and septic rat models. However, the biological composition of human ISF is more complex due to the influence of diseases and medications, so the specificity of the microneedle platform surface requires further clinical validation in real-world applications (Fig. 1b). Zheng et al.[26] developed a microneedle patch by mixing methacrylate-modified hyaluronic acid (MeHA) and hyaluronic acid (HA), which was coupled with a four-channel electrochemical sensor array with different response mechanisms. This "microneedle coupled electrochemical sensor array (MNESA)" achieved continuous measurement of four biomarkers in ISF-phosphate, urea, creatinine, and uric acid-and demonstrated a high correlation between ISF measurements and results from commercial serum kits. The combined analysis of these four indicators significantly reduces the risk of overlooking early-stage chronic kidney disease (CKD) and the subsequent progression of renal function impairment and renovascular lesions (Fig. 1c). As the spectrum of detectable analytes broadens to encompass ion concentrations, glucose, antibiotics, cholesterol, pH, and miRNA[27–32], flexible microneedle platforms are poised to become a leading frontier in flexible sensing technologies for the preoperative diagnosis of panvascular disease.

In the future, the "lab-on-a-microneedle" design[33] may become one of the optimization pathways for flexible microneedle platforms (Fig. 1d). This

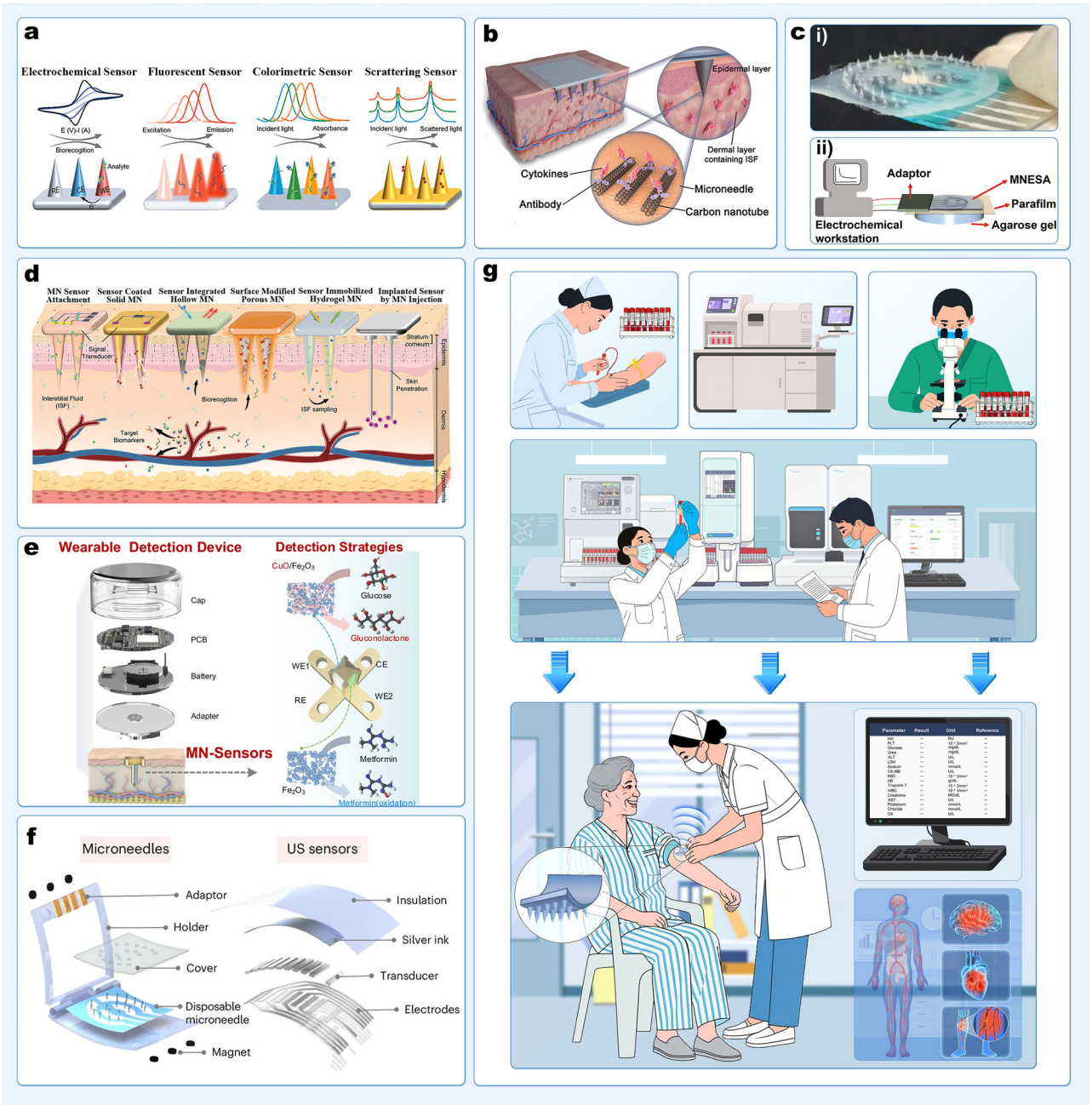


Fig. 1 | Flexible microneedle platforms poised to reshape the paradigm of laboratory testing for panvascular diseases. a Various flexible microneedle platforms based on different sensing principles. Reproduced with permission[23]. Copyright © 2024, John Wiley and Sons. **b** Schematic diagram of the working mode of a flexible microneedle platform utilizing a functionalized surface to monitor IL-6 levels in mouse ISF. Reproduced with permission[25]. Copyright © 2023, John Wiley and Sons. **c** (i) Optical image of the microneedle coupled electrochemical sensor array (MNESA). (ii) microneedle coupled electrochemical sensor array (MNESA): Schematic diagram of a flexible microneedle platform monitoring biomarkers in an artificial skin model via electrochemistry. Reprinted with permission[26]. Copyright © 2023, Elsevier. **d** Schematic diagram of the working principle of a flexible microneedle platform based on "lab-on-a-microneedle" design. Reproduced with permission[23]. Copyright © 2024, John Wiley and Sons. **e** Microneedle-based Continuous Biomarker/Drug Monitoring (MCBM) system: Schematic diagram of a flexible microneedle platform utilizing nanozyme coatings to monitor glucose and metformin concentrations in diabetic patients. Reproduced with permission[34]. Copyright © 2025, Springer Nature. **f** biomarkers-linked ultrasound electronic (BLUE) platform: Structural schematic of a flexible microneedle platform utilizing ultrasonic sensors within a flexible substrate to monitor biomarkers. Reproduced with permission[38]. Copyright © 2025, Springer Nature. **g** Schematic diagram illustrating the paradigm shift from traditional blood-based laboratory testing to interstitial fluid (ISF)-based laboratory testing.

will require innovative thinking and a comprehensive comparison of different sensing strategies. Yang et al.[34] developed a Microneedle-based Continuous Biomarker/Drug Monitoring (MCBM) system featuring microneedle electrodes modified with nanozyme coatings—specifically, Fe_2O_3/CuO for glucose sensing and Fe_2O_3 for metformin sensing. Upon the entry of specific substrates into the two working electrodes via four microchannels, differential pulse voltammetry (DPV) facilitates electrocatalytic oxidation at the coating surface, generating characteristic current signals. These signals not only reflect blood glucose and metformin concentrations but also facilitate real-time pharmacokinetic and pharmacodynamic analysis of metformin. Such an electrochemical sensing strategy significantly ensures the real-time responsiveness of "lab-on-a-

microneedle" measurements (Fig. 1e). Conversely, Ranamukhaarachchi et al.[35] functionalized the inner lumen surfaces of hollow microneedles with specific ligands to capture target molecules. By integrating this setup with an optofluidic biosensor, they achieved absorbance measurements with a high signal-to-noise ratio. The experimental limit of detection for vancomycin reached as low as 84 nM, significantly superior to the 1.35 μM threshold of commercial kits. Although not implemented on a flexible substrate, this optical sensing strategy underscores the potential for high precision and sensitivity in "lab-on-a-microneedle" applications. Constrained by platform size and the corresponding limited detectable sample volume[36], further enhancements in detection sensitivity and precision remain critical for flexible microneedle platforms to effectively replace large-scale laboratory analytical instruments. With deeper exploration of Raman spectroscopy and the development of portable, handheld surface-enhanced Raman spectrometers, surface-enhanced Raman scattering (SERS) sensing technology may become a highlight for point-of-care testing at nanomolar or picomolar levels[37]. Furthermore, Chang et al.[38] achieved multimodal analysis within a "lab-on-a-microneedle" framework by synergistically monitoring physical and chemical signals on a flexible microneedle array. Their developed biomarkers-linked ultrasound electronic (BLUE) platform is capable of not only quantifying multiple metabolites in ISF but also measuring arterial diameter changes at the wrist via integrated ultrasound sensors. Through calibration algorithms, these data are converted into blood pressure waveforms to evaluate cardiovascular risk metrics such as arterial elasticity. Additionally, continuous monitoring of heart rate and electrocardiograms using biopotential electrodes printed with custom silver ink offers significant value for vascular assessment in the Assessment stage. This ultrasound-based sensing strategy presents a viable pathway for the multifunctional evolution of future "lab-on-a-microneedle" systems (Fig. 1f).

Additionally, the specifications of the microneedles (height, width, aspect ratio), tip geometry, and insertion depth and angle can all affect the accuracy of real-time monitoring[21]. Therefore, the flexibility of these platforms for use on different body parts must be enhanced.

Flexible microneedle platforms will provide patients with panvascular disease with point-of-care preoperative diagnostics that are on par with traditional blood analysis, reshaping the paradigm of laboratory testing through the integration of flexible sensing devices (Fig. 1g). This is an indispensable component of the Assessment stage in the "4 A Tetrahedron System". (Fig. 1)

"Smart" design of interventional devices with flexible sensors

While focusing on patient diagnosis and testing, the Assessment stage of the "4 A Tetrahedron System" also emphasizes the evaluation of interventional devices and the integration of flexible sensors.

The balance of three major ecosystems-mechanical, cellular, and physicochemical-immune—is a key criterion for assessing vascular health and a crucial indicator for evaluating the "suitcordance"[6] of interventional devices, especially their long-term concordance with the vessel.

- The maintenance of *mechanical* ecosystem balance primarily depends on changes in vascular stress under the influence of hemodynamics, including tangential shear stress, radial and circumferential pressure, and longitudinal tensile forces on the vessel wall[39].
- *Cellular* ecosystem balance relies on the efforts of vascular endothelial cells, smooth muscle cells, and fibroblasts[40–42] in maintaining the normal structure and function of the vessel.
- The physicochemical-immune ecosystem balance pertains to the dynamic regulatory interplay among the intravascular physicochemical environment (e.g., temperature, pH), lipid metabolism (e.g., subendothelial retention of LDL[43]), and immune responses (e.g., secretion of pro-inflammatory cytokines such as IL-1β and IFN-γ).

Currently, widely employed clinical interventional devices-including vascular stents, artificial heart valves, and cardiac occluders-share a critical limitation: the inability to rapidly detect postoperative complications. We propose the definition of "smart interventional devices", which are typified by the integration of novel flexible sensors into conventional interventional devices. With the core objective of enhancing the "suitcordance" of panvascular interventional devices, these systems leverage the in situ, real-time, and continuous monitoring capabilities of flexible sensors to mitigate postoperative risks and improve prognostic outcomes. Notably, this "smart" capability is realized through implantable flexible sensors—specifically those directly integrated with the interventional device itself, rather than solely interfacing with the vessel wall or tissue structures. Within the "4 A Tetrahedron System", the design and refinement of "smart interventional devices" constitute a critical component of the Assessment stage. This is because such devices must not only promptly restore normal hemodynamics intraoperatively but also ensure the patient's long-term postoperative vascular status. Only through the rational selection and design of flexible sensors can conventional tools be transformed into "smart interventional devices" with superior suitcordance, without compromising their intrinsic interventional functions.

Using vascular stents as an example, the risks arising from imbalances and discordance among the mechanical, cellular, and physicochemical-immune ecosystems at the stent-vessel interface remain undetectable with sufficient timeliness and accuracy, thereby posing latent threats of adverse events such as in-stent restenosis[44] and late lumen loss[45] following intervention. Flexible sensors can quantify physical parameters (e.g., temperature, pH, osmotic pressure), biochemical parameters (e.g., lactate, glucose), and kinetic parameters (e.g., pressure, flow rate) of blood flow. This endows "smart stents"[46–48] (Fig. 2a–c) with the capability for continuous in situ monitoring at the lesion site and establishes a framework for assessing the restoration of the three primary vascular ecosystems—mechanical, cellular, and physicochemical-immune[49]—post-intervention.

A vascular stent integrated with flexible sensors, designed by Wang et al.[50], serves as a reference template for the design of "smart stents". This wireless LC (inductor-capacitor) pressure sensor features a multi-layer design, including a novel Perminex layer. In phantom system tests, it demonstrated a seven-fold increase in sensitivity for cardiovascular hemodynamic monitoring under the same pressure. However, the lack of in-vivo research data is a major obstacle to its clinical translation. Further evaluation is needed to determine if existing filtering strategies can effectively suppress noise interference from cardiac pulsations and respiratory movements within the panvascular system to prove its feasibility for in-vivo applications. In the future, we hope to see more flexible sensors related to vascular stress integrated with "smart stents". For example, the flexible tensile strain-pressure sensor designed by Xu et al.[51], can independently detect in-plane tensile force and out-of-plane pressure. Its unique serpentine geometry not only ensures off-axis sensing insensitivity to enhance the effectiveness of decoupling tensile force and pressure but also exhibits resilient compliance that is highly compatible with vascular mechanics. Further exploration of its integration with vascular stents, based on in vivo validation, represents a highly attractive development direction for "smart stents" in monitoring the mechanical ecosystem balance in panvascular disease.

Future flexible sensors also need to target common vascular lesion characteristics across various panvascular diseases, using biomarkers related to abnormal pathological phenomena such as immune cell accumulation and smooth muscle proliferation as monitoring indicators. Flexible Graphene Field-Effect Transistors (GFETs)[52] overcome the limitations of traditional silicon-based materials, which lack flexibility and stretchability. They not only lead in the detection of large biomolecules like proteins and nucleic acids-by using antigen-antibody recognition to detect prostate-specific antigen[53] (Fig. 2f) and by using specific base sequences conjugated on the graphene channel to recognize and bind miRNA[54] -but can also monitor small molecules such as cytokines. For instance, Hao et al.[55] immobilized a single-stranded oligonucleotide named Aptamer VR11 on a graphene surface, which folds into a guanine quadruplex structure to enhance its specific affinity for TNF-α. Its response sensitivity and mechanical flexibility were validated in preliminary experiments. Similarly, Chen et al.[56] developed a DNA-functionalized flexible GFET sensing device

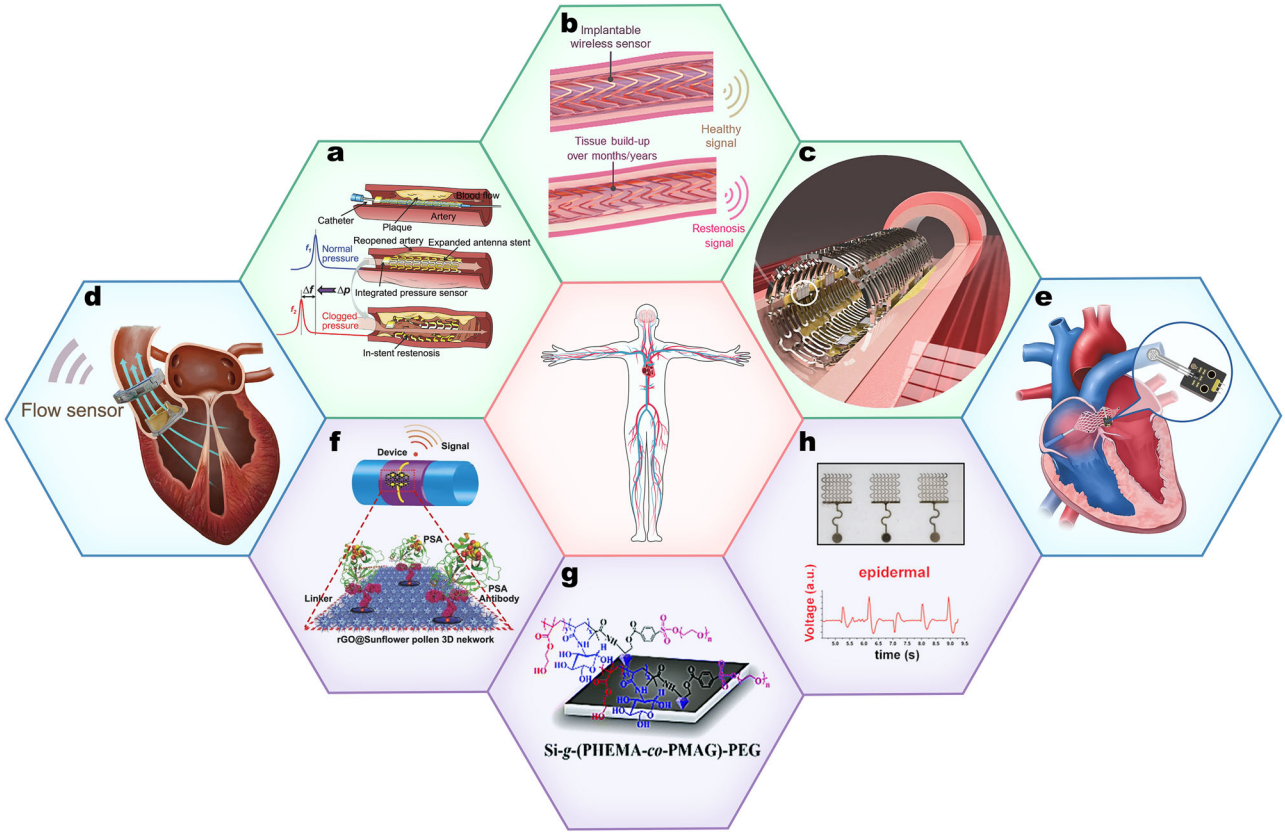


Fig. 2 | "Smart interventional devices" integrated with flexible sensors. **a** Schematic of a "smart stent" for detecting in-stent restenosis and occlusion. Integrated micro-pressure sensors can monitor the RF resonant frequency of the target site in real-time, warning of in-stent restenosis and occlusion via a handheld RF converter. Reproduced with permission[46]. Copyright © 2018, John Wiley and Sons. **b** Implantable bioelectronic systems related to "smart stents" for detecting in-stent restenosis. Reproduced with permission[47]. Copyright © 2023, Elsevier. **c** Workflow diagram of a "smart stent" for remotely detecting endothelialization progress and warning of in-stent restenosis. Implantable bioimpedance sensors are integrated at multiple points on the stent body, completing data telemetry via a miniature wireless impedance analyzer. Reproduced with permission[48]. Copyright © 2022, John Wiley and Sons. **d** Working schematic of a "smart artificial heart valve". By connecting a magnetic flow sensor to the ascending aorta segment, the characteristic curve of blood flow downstream of the aortic valve is measured. Reproduced with permission[66]. Copyright © 2020, Public Library of Science. **e** Future outlook for a "smart atrial septal occluder" with flexible sensors integrated on the disc surface. **f** A flexible Graphene Field-Effect Transistor (GFET) sensor working on the principle of antigen-antibody recognition, capable of specifically detecting prostate-specific antigen, which holds promise for application in "smart stents". Reproduced with permission[53]. Copyright © 2016, John Wiley and Sons. **g** An antifouling functionalized surface constructed based on poly(2-hydroxyethyl methacrylate)(PHEMA) materials, which is expected to solve the problem of long-term non-specific biomarker fouling of "smart interventional devices". Reprinted with permission[58]. Copyright © 2020, Royal Society of Chemistry. **h** Epidermal flexible sensors capable of measuring strain, skin bioimpedance, and heart rate. These holds promise for future integration with atrial septal occluders to realize the design goal of a "smart occluder". Reprinted with permission[69]. Copyright © 2020, American Chemical Society.

that indirectly measures VEGF concentration based on its differential affinity for different DNA strands. It exhibits excellent performance with a low limit of detection for VEGF165. This method of amplifying detection signals through a hybridization chain reaction can be extended to other small molecules, showing broad innovative potential in panvascular disease. While the achievements of flexible GFET sensors in cytokine monitoring are commendable, their integration with "smart stents" must overcome the bottleneck of long-term stability. This stability is compromised by a multitude of factors. On one hand, functionalized coatings must withstand non-specific biomarker fouling during months or even years of exposure to the hemodynamic environment. With the research and synthesis of nonionic polymers (e.g., poly(oligo(ethylene glycol) methyl ether methacrylate) (POEGMA)[57], poly(2-hydroxyethyl methacrylate) (PHEMA)[58]) (Fig. 2g) and zwitterionic polymers (e.g., poly(2-methacryloyloxyethyl phosphorylcholine) (PMPC)[59], poly(sulfobetaine methacrylate) (PSBMA)[60]), the physical integration and functional independence of flexible GFET sensor surfaces with antifouling polymer brush coatings becomes a common prerequisite for their monitoring of vascular cellular and physicochemical-immune ecosystems. However, biological macromolecules in the blood, such as lipoproteins and fibrinogen, may still compromise coating integrity through hydrophobic interactions or charge accumulation. Furthermore, immune cells recruited by the inflammatory response at the lesion site can accelerate the biodegradation of these coatings via reactive oxygen species (ROS) attacks[52]. On the other hand, electrochemical oxidation at the graphene-electrolyte interface is inevitable. This phenomenon induces a drift in the Dirac point, leading to baseline instability in sensor signals and thereby compromising readout reliability. Particularly during prolonged operation, the gate dielectric layer is prone to permeation due to extended immersion in ion-rich body fluids. This not only alters the properties of the dielectric layer but may also trigger irreversible degradation of the graphene channel. Concurrently, the potential of the reference electrode is subject to fluctuations caused by material consumption and surface passivation, which further exacerbates measurement errors.

To further overcome the impediment of the imbalance between traditional vascular stents and the body's mechanical, cellular, and physicochemical-immune ecosystems, bioresorbable stents show broad development prospects, driven by continuous innovation in novel polymer materials. However, during their "smart" integration with implantable, degradable flexible sensors, they face the core issue of mismatched degradation profiles of different materials. For example, the polylactic acid, the

main material of the XINSORB bioresorbable stent, takes four to five years to degrade completely[61], whereas the lifespan of degradable sensing devices is often measured in "months" or even "days"[62]. This disparity in degradation rates could not only lead to the premature loss of the stent's electronic monitoring function but also hinder the harmless absorption of the degradable electronic components. Furthermore, influenced by factors such as material structure, elements, content, and surface functionalization, the biocompatibility of 2D materials like graphene-based materials and transition metal dichalcogenides has not yet been standardized quantitatively. There is a lack of research on cytotoxicity mechanisms and experiments on tissue immune responses[63], which poses a severe challenge to the biocompatibility of packaging materials for long-term degradable flexible sensors and their interaction with the vascular microenvironment.

Beyond the reliance on in situ data monitoring via flexible sensors, advanced dynamic imaging technologies have demonstrated significant potential in assessing the interfacial interactions between "smart stents" and the vessel wall. For instance, Sun et al.[64] demonstrated that synchrotron radiation CT effectively mitigates the blooming and beam hardening artifacts inherent to conventional CT, thereby providing robust technical support for the precise diagnosis of calcified lesions. Similarly, Ginn-Hedman et al.[65] elucidated the advantages of diffusible contrast-enhanced micro-CT in enhancing post-implantation stent visualization. This technique significantly reduces artifacts induced by metallic stents, thereby mitigating the overestimation of restenosis severity caused by luminal edge blurring. Collectively, synchrotron radiation and micro-CT enable the characterization of the stent's in vivo status with micron-level spatial resolution and millisecond-level temporal resolution. These modalities facilitate the dynamic visualization of stent expansion morphology, strut-vessel wall apposition, and the local hemodynamic environment under physiological flow conditions. By observing minute displacements of stent struts and the local strain distribution of the vessel wall, these technologies allow for the timely monitoring of mechanical ecosystem shifts at the device-vessel interface. To strictly validate the 'suitcordance' of these smart devices, advanced operando characterization techniques are indispensable. Emerging technologies, such as Advanced Synchrotron Radiation and Micro-Computed Tomography (Micro-CT), offer high-resolution, non-destructive visualization of the device-vessel interface. Unlike traditional static histology, these methods enable the precise assessment of stent strut apposition, endothelialization progress, and mechanical integrity under dynamic flow conditions. Incorporating such operando characterization into the Assessment stage will provide a rigorous feedback mechanism for optimizing the structural design and biocompatibility of future smart interventional devices.

The design of future "smart stents" will also require technological breakthroughs in the integration of multi-modal flexible sensors to enhance the monitoring of multi-dimensional information, such as stress distribution differences and cytokine concentrations, thereby achieving a "re-balancing" of the mechanical, cellular, and physicochemical-immune ecosystems between the device and the vessel post-intervention, further improving the "suitcordance" between the interventional device and the human body.

Beyond their role in "smart stents", flexible sensors will also contribute to the design of other "smart" panvascular interventional devices. Vennemann et al.[66] implanted a magnetic flow sensor in the ascending aorta to enable real-time remote monitoring of blood flow characteristics downstream of an artificial valve after aortic valve replacement (Fig. 2d). However, the turbulent fluctuations and vortex velocity components of blood flow from the left ventricle to the ascending aorta limit the precision of flow measurement. In the future, integrating thinner flexible film sensors and reducing the spatial gap between the sensing device and the artificial valve to promptly detect changes in cardiac output could be a promising direction for the design of "smart" artificial heart valves. Following transcatheter atrial septal defect and patent foramen ovale closure, late-stage embolus formation is considered a high-risk delayed complication[67]. Dislodged emboli can travel through the bloodstream to coronary, cerebral, renal, or lower limb arteries, potentially causing acute complications like myocardial infarction, stroke, renal artery embolism, or lower limb ischemia. This poor sealing effect may be related to residual shunts caused by perforation or dissolution of the polymer membrane on the occluder discs, as well as delayed endothelialization[68]. Integrating distributed flexible strain sensors and bioimpedance sensors[69] (Fig. 2h) on the left and right discs could allow for timely monitoring of the integrity of the polymer membrane and the degree of endothelialization. Meanwhile, integrating flexible pressure sensors or micro-flow sensors at the waist of the occluder could enable real-time assessment of its support performance and prevent residual shunts, providing ideas for the future "smart" design of cardiac occluders (Fig. 2e).

In the future, multi-modal flexible sensor integration strategies will endow panvascular interventional devices with rich in-situ "smart" sensing capabilities, providing them with continuous monitoring functions of the lesion microenvironment. This will, in turn, offer a dynamic quantitative evaluation system for the reconstruction of the "three homeostatic ecosystems"—mechanical, cellular, and physicochemical-immune—after panvascular interventional therapy. The integration of flexible sensors will also greatly enhance the suitcordance of traditional interventional devices, thus providing a power source for shaping the concept of the "4 A Tetrahedron System", which utilizes flexible electronic devices to improve the entire process of panvascular disease interventional therapy (Fig. 2).

Within the "base" of the "4 A Tetrahedron System", the Assessment stage's evaluation of the patient's condition and the device's functionality is critical to the success of panvascular interventional therapy. With the help of flexible sensing devices, flexible microneedle platforms can store pathological features obtained from ISF analysis in a personalized "electronic file". This information, along with imaging diagnostic results, provides valuable guidance for selecting surgical methods in the Assistance stage. It also facilitates remote data access during the Aftercare stage, offering a reference for rehabilitation prediction and the formulation of recuperation strategies. Interventional devices integrated with flexible sensors will be directly applied in the operational procedures of the Assistance stage, improving surgical quality and success rates while reducing the risk of postoperative complications in the Aftercare stage. With hyperglycemia becoming increasingly severe, diabetic foot-a prominent manifestation of panvascular disease in the lower limbs and feet, and a serious consequence of diabetic complications caused by peripheral vascular lesions-increasingly requires sufficient attention. The "4 A Tetrahedron System", built around the "Assessment-Assistance-Aftercare" base, is poised to provide a full-process reference solution covering diagnosis, treatment, and prognosis for diabetic foot patients from a macroscopic systemic perspective. For example, in a patient with a diabetic foot, a flexible microneedle platform can be applied near the ulcerated, infected, or even gangrenous area to detect ISF glucose and inflammatory cytokine levels, with the data recorded in the cloud (Assessment). Based on this data and preoperative CT imaging, the physician diagnoses the cause as insufficient blood supply to the foot due to hyperglycemia-induced infrapopliteal artery stenosis. A "smart stent" is then implanted in the infrapopliteal artery via a femoral approach, with the flexible sensor providing real-time feedback on wall apposition and surgical progress (Assistance). During the prognosis period, ISF glucose levels are compared with the cloud data to adjust the dosage of hypoglycemic medic AI-retrofitation. The "smart stent" within the patient can sense thrombus formation in real time, alerting the patient through signal changes to seek timely follow-up and treatment plan adjustments (Aftercare). Flexible electronic devices assist the Assessment stage in achieving ISF-centered biomarker quantification and interventional device optimization, which is a crucial prerequisite for establishing the triangular circulation of the "base" of the "4 A Tetrahedron System".

Assistance: radiation-free imaging guidance & sub-millimeter magnetic navigation

Guidewires and catheters, commonly used instruments in panvascular interventional therapy, often face challenges such as weak steering capability, low maneuverability, and poor stability within blood vessels[70]. This

necessitates reliance on large, high-resolution imaging systems and places high demands on the physician's operational skill and precision. The complex vascular anatomy of patients with panvascular disease typically requires intricate and tedious guidewire manipulation, which translates to increased doses of contrast agents, adding to the patient's renal burden, and longer radiation exposure[71]. It also implies a higher risk of accidental events such as endothelial damage, vessel rupture, perforation, or even intraoperative dissection due to improper handling[72,73]. The Assistance stage of the "4 A Tetrahedron System" emphasizes the role of flexible electronic devices in guiding intraoperative panvascular interventions. The aim is to utilize high-resolution imaging to observe the real-time position of the guidewire/catheter while avoiding X-ray radiation and the burden of contrast agents. Simultaneously, it aims to improve the design of the guidewire/catheter itself, endowing it with sub-millimeter steering and automatic navigation capabilities to achieve the ultimate objective of making the interventional process more convenient and safer.

The goal of the Assistance stage is to leverage flexible electronic systems to ensure the precise execution of the interventional plan, thereby establishing the initial conditions for optimal short-term suitability and long-term concordance.

Flexible ultrasonic transducer arrays to enhance interventional guidance imaging systems

Ultrasound/photoacoustic imaging systems, with ultrasonic transducers as their key component, have become a mainstream choice in medical diagnostics and industrial inspection due to their deep structural detection capabilities, ease of operation, and high efficiency[74–76]. Miniaturized, high-density flexible ultrasonic transducer arrays, as the core sensing units of these systems, have been widely applied in clinical imaging[77,78]. If further applied to interventional guidance, they would demonstrate the powerful assistance capabilities of flexible electronic devices in the intraoperative navigation of panvascular interventional therapy. Ultrasound/photoacoustic imaging technology assisted by flexible ultrasonic transducer arrays can obtain intuitive vascular data while guiding interventions. By guiding the analysis of the patient's luminal environment and the three major ecosystems (mechanics, cellular, and physicochemical-immune), it enhances the suitcordance-especially long-term concordance-between the interventional device and the vessel, aiming to achieve the long-term shared destiny of the device and the human body.

Flexible ultrasound patches based on flexible ultrasonic transducer arrays are a significant step in the miniaturization of ultrasound imaging systems. The Bioadhesive ultrasound patch designed by Wang et al.[79] assembles an ultrathin ultrasound probe with a hydrogel-elastomer coupling layer. It boasts multi-center frequency elements (3, 7, 10 MHz), high axial resolution (0.77 mm, 0.225 mm, 0.1924 mm), and high bandwidth (68%, 75%, 78%), enabling 48-hour continuous imaging of various vessels, including the carotid artery, jugular vein, heart, and stomach (Fig. 3d). However, its reliance on large external processing systems remains a point for consideration. The ultrasonic-system-on-patch (USoP) designed by Lin et al.[80] addresses this issue. First, a PZT-5H piezoelectric layer is connected to anisotropic conductive films via serpentine circuits to form the ultrasound probe. Then, a miniaturized wireless control circuit, designed with an "analog front-end (AFE) + data acquisition module (DAQ)", handles high-frequency signal processing, 12 MHz high-speed sampling, and 3.4 Mbps wireless transmission. Finally, an AI algorithm enables imaging display on a smartphone app connected to a cloud server, achieving a "fully integrated" system for data acquisition, conversion, and analysis without dependence on external equipment (Fig. 3a). Flexible ultrasound patches, created by embedding micro-fabricated flexible ultrasonic transducer arrays into flexible substrates, exhibit excellent tissue conformity and wearability[81–83], contributing significantly to the miniaturization of ultrasound imaging systems[84–87] (Fig. 3b, c, e, f). Currently, ultrasound imaging systems have overcome the traditional trade-off between penetration depth and resolution, achieving remarkable success in independently guiding procedures like transcatheter mitral valve edge-to-edge repair, structural heart disease treatment, and atrial fibrillation catheter ablation using techniques like echocardiography and intracardiac ultrasound[88–90]. It is hoped that future ultrasound imaging systems based on flexible patches will solve the challenges of high frequency, high power consumption, and high bandwidth, break through the bottleneck of balancing size and function, and inject new vitality into the development of miniaturized interventional guidance imaging systems.

The application of flexible ultrasonic arrays in photoacoustic imaging probes will allow photoacoustic imaging to combine the high contrast of traditional optical imaging with the deep penetration of ultrasound, offering a reasonable prospect for intraoperative imaging guidance. Wang et al.[91] invented a fully flexible photoacoustic coupling system that integrates a 128-element flexible ultrasound probe and an optical shape-sensing (OSS) flexible fiber bundle. Building on the advantage of optical contrast, this system improves the imaging resolution of photoacoustic tomography to 130 micrometers, which generally meets the resolution requirements for vascular interventional guidance. The 3D photoacoustic scanner designed by Huynh et al.[92] is based on a Fabry-Perot (FP) polymer film ultrasonic transducer. By combining high pulse repetition frequency (PRF) excitation lasers and compressed sensing techniques, it shortens the device's response time, significantly enhancing the efficiency of photoacoustic tomography (PAT) and enabling dynamic 3D imaging of microvasculature (Fig. 3g). These advancements demonstrate the promising future of photoacoustic imaging in interventional guidance, but numerous limitations for clinical application still exist. A low imaging frame rate, leading to insufficient real-time capability, is a critical flaw that restricts the application of photoacoustic imaging in this field. Especially when facing the high-precision demands of procedures like coronary intervention, the inability to display the position of the guidewire/catheter tip in time can exacerbate the risk of intraoperative complications such as vessel perforation and dissection. Photoacoustic imaging relies on ultrasonic signals generated after a laser penetrates tissue. When imaging deep vessels like the aorta or in obese patients, laser scattering and a reduced signal-to-noise ratio in ultrasound reception can lead to blurred vessel contours. Particularly in brain imaging, the obstruction of the skull limits laser penetration, potentially causing imaging failure[93]. Despite its immense technical potential, the clinical validation of photoacoustic imaging in interventional procedures remains in its nascent stages. In the realm of panvascular disease, the pivotal advantage of photoacoustic imaging lies in the identification of vulnerable plaques. While established modalities such as coronary angiography, intravascular ultrasound (IVUS), and optical coherence tomography (OCT) excel at delineating vascular anatomy, they offer limited capability in assessing plaque stability. In contrast, photoacoustic imaging can reveal critical compositional features—such as lipid cores and inflammatory activity—by mapping the distribution of endogenous chromophores like hemoglobin. This capability is of paramount importance for the predictive risk stratification of acute vascular events. However, translating this potential into routine clinical practice is fraught with challenges. Specifically, interventional applications demand higher imaging frame rates to synchronize with the cardiac cycle, further miniaturization of catheters to navigate the coronary lumen, and operational stability within the dynamic hemodynamic environment. These unresolved technical impediments constitute the primary bottlenecks currently restricting its widespread clinical adoption. Currently, photoacoustic imaging systems have applications in static imaging fields such as tumor diagnosis, vascular structure and function assessment, cardiovascular atherosclerosis evaluation[94], and peripheral vascular visualization[95,96] (Fig. 3h,i). However, there is still a significant gap to bridge before it can be used, either alone or in combination with ultrasound, to guide interventions (Fig. 3).

Furthermore, the continuous improvement of flexible ultrasonic arrays will be a significant driving force for advancing ultrasound/photoacoustic imaging-guided interventions. Existing backing layer materials, such as polyimide PCBs (Kapton PCB) and flexible polyurethane rubber with tungsten particles, struggle to balance the two desirable properties of high acoustic attenuation and flexibility[97,98]. It is necessary to develop new

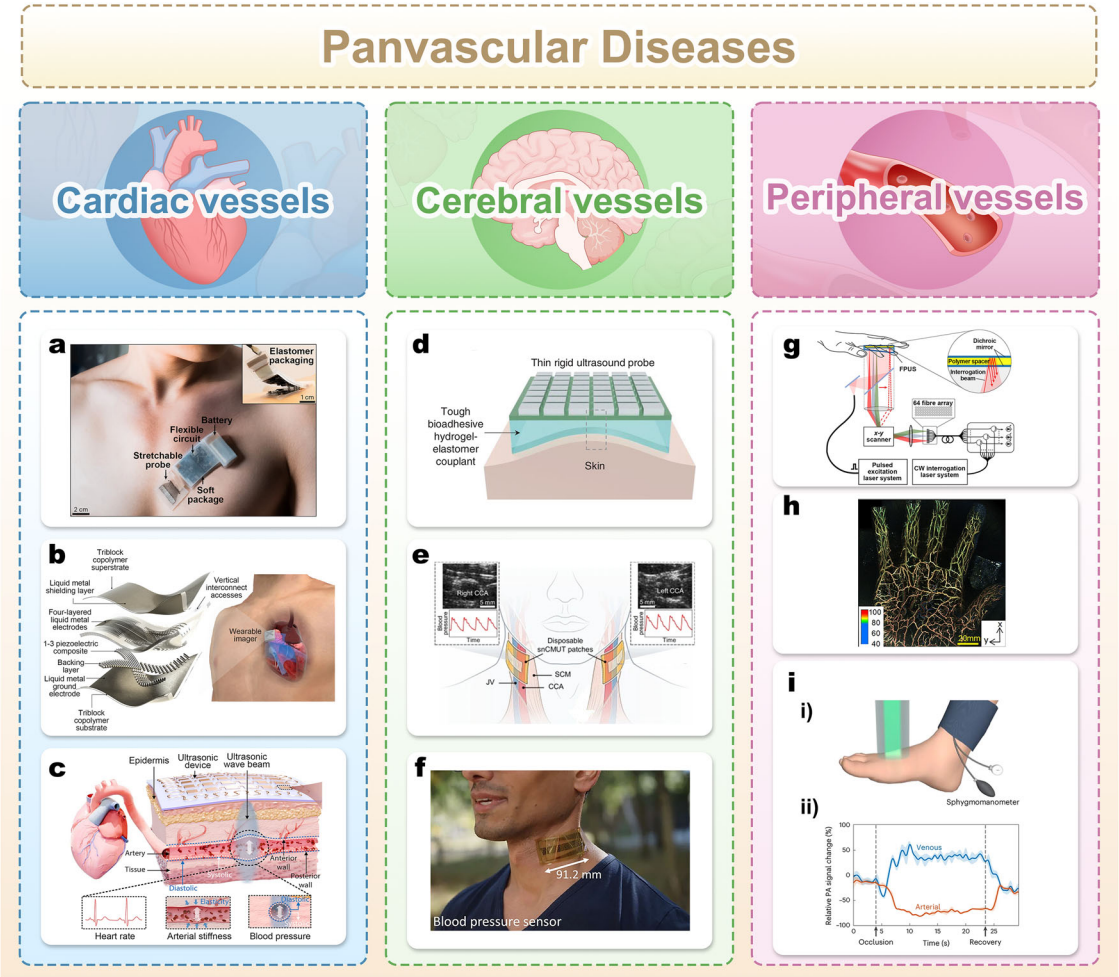


Fig. 3 | Applications of ultrasound/photoacoustic imaging technology based on flexible ultrasonic transducer arrays in the panvascular field. a Construction of the ultrasonic-system-on-patch (USoP) attached to the chest, capable of continuous monitoring of cardiac activity and B-mode imaging. Reprinted with permission[80]. Copyright © 2024, Springer Nature. **b** A design of a wearable cardiac imager, capable of cardiac B-mode imaging and echocardiogram observation. Reprinted with permission[84]. Copyright © 2023, Springer Nature. **c** Flexible ultrasonic transducer arrays for cardiovascular dynamic parameter measurement. Reprinted with permission[85]. Copyright © 2025, American Association for the Advancement of Science. **d** Bioadhesive ultrasound (BAUS) device capable of long-term continuous imaging of the common carotid artery and jugular vein. Reprinted with permission[79]. Copyright © 2022, The American Association for the Advancement of Science. **e** B-mode imaging for the common carotid artery and jugular vein, and M-mode imaging of the pulsation pattern of CCA walls by disposable snCMUT patches. Reprinted with permission[86]. Copyright © 2025, Springer Nature. **f** Flexible ultrasonic transducer arrays for carotid blood pressure measurement and B-mode imaging. Reprinted with permission[87]. Copyright © 2024, Springer Nature. **g** Structural schematic of Multibeam FP-based PAT scanner, capable of high-resolution photoacoustic imaging scanning of fingertips. Reprinted with permission[92]. Copyright © 2024, Springer Nature. **h** Visualization of hand blood vessels achieved through high-resolution and large-area photoacoustic imaging. Reprinted with permission[95]. Copyright © 2018, Springer Nature. **i** (i) Schematic diagram of using photoacoustic computed tomography (PACT) with ergodic relay (ER) for foot scanning imaging. (ii) Relative PA signal change curves for foot arteries and veins from the PACTER system; hemodynamic data can be utilized to guide the prevention of peripheral vascular diseases. Reprinted with permission[96]. Copyright © 2023, Springer Nature.

composite backing layer materials that can prevent interference from acoustic energy radiated backward from the piezoelectric element while ensuring good conformity with the curved surfaces of human skin. The acoustic matching layer of flexible ultrasonic arrays should adopt a gradient impedance multi-layer design, with the thickness (d) of each layer strictly satisfying the resonance condition $d = \lambda/4$ (where λ is the wavelength corresponding to the center frequency of the nth layer). On this basis, the effects of parameters like density on acoustic wave transmission should be further compared. Unlike traditional media, the acoustic impedance of the vessel wall exhibits dynamic, non-uniform changes. Therefore, the material selection for the matching layer must also be enhanced to adapt to the acoustic properties of the vessel wall, reducing ultrasound reflection and improving energy transfer efficiency by progressively minimizing the acoustic impedance difference between the piezoelectric element and the acoustic lens.

Compared to the current gold standard for panvascular intervention, DSA, ultrasound/photoacoustic imaging systems offer the advantages of being free from radiation damage and contrast agent burden. Further exploring their feasibility in the field of interventional guidance imaging will become a new track with enormous potential.

Flexible magnetic navigation devices for precise intraoperative guidance

In contrast to the invasive approaches of open-chest or open-skull surgery, the precise delivery of guidewires/catheters is the core technical aspect of minimally invasive interventional therapy. However, the delivery of these instruments faces severe challenges in panvascular practice. In patients with a type III aortic arch, where the apex of the arch is lowered and acutely angled, guidewire delivery for carotid artery stenting is often difficult, with catheters frequently entering branch vessels, sometimes leading to surgical

failure[99]. In coronary chronic total occlusions (CTO) or severely calcified arteries, there may be tortuous microchannels smaller than 200 μm in diameter, which are encapsulated by calcified lesions larger than 2 mm, forming a false lumen and making it difficult for the guidewire to find the true lumen[100]. A more critical conflict exposed in clinical practice is that while high-stiffness guidewires have enhanced pushability, they also have a greatly increased risk of vessel perforation. Conversely, flexible catheters have a lower probability of causing vessel damage but lose manipulative precision due to attenuated torque transmission. Against this backdrop, the versatile and integrated application of flexible magnetic navigation devices and surgical robot systems provides real-time feedback with sub-millimeter deflection accuracy, enabling precise directional control within complex anatomical structures. Combined with intelligent propulsion control assisted by a robotic arm, this further enhances the stability of interventional operations. The precise guidance role of flexible magnetic navigation devices is a key function in interventional guidance, making them a core participant that deeply empowers the Assistance stage of the "4 A Tetrahedron System".

Unlike the ultrasound/photoacoustic imaging approaches described in the interventional guidance imaging section, which focus on visualizing the vascular environment but lack actuation capability, flexible magnetic navigation provides active steering and propulsion but relies on external imaging modalities for feedback. The precise guidance role of flexible magnetic navigation devices is a key function in interventional guidance, making them a core participant that deeply empowers the Assistance stage of the "4 A Tetrahedron System".

Based on the traditional definition of "flexible electronics technology", whether flexible magnetically controlled guidewires/catheters fall into this category remains a controversial topic. Although the method by which flexible magnetic guidewires/catheters achieve deflection relies only on the torque generated by the permanent magnet at the tip in response to external magnetic field changes, rather than on electronic devices or circuits built on flexible substrates, their ability to achieve benign interaction with the human body through advantages such as bendability, biocompatibility, miniaturization, and integration aligns with the design philosophy and basic principles of flexible electronic devices. In recent years, the rise of concepts such as soft robotics[101] and continuum robotics[102] has created opportunities for the further combination of flexible magnetic control devices and flexible electronics. Through integration with flexible sensors and artificial intelligence algorithms, magnetic navigation devices will be endowed with intelligent capabilities for information acquisition, processing, and transmission. In the Assistance stage of the "4 A Tetrahedron System", based on the auxiliary capability of precise intervention, establishing a comprehensive flexible electronic surgical robot system with stronger patient vascular personalization and higher device-human suitcordance will unleash greater potential for magnetic navigation devices.

Flexible magnetic navigation devices have broad application prospects in the interventional treatment of panvascular (cardiac, cerebral, peripheral) diseases. The use of magnetic-guided ablation catheters for the treatment of cardiovascular conditions like arrhythmias and atrial fibrillation[103–105] is already relatively mature. In the future, constructing flexible magnetic actuation units from magnetic hydrogels[106] or magnetic flexible metastructures[107], and integrating a flexible temperature-sensing layer at the tip holds the promise of transitioning from "partial flexibility" of the catheter's main polymer material to "full flexibility". R. Dreyfus et al.[108]. designed a helical protrusion on the surface of a soft magnetic guidewire, which overcomes the problem of insufficient propulsion force during long-distance delivery and enhances accessibility in tortuous vessels. They successfully navigated from a radial artery approach, through a 90° "knee" bend in the distal M1 segment of the middle cerebral artery, to reach the M2 segment in a porcine model. This product can also achieve precise positioning and crossing of aneurysm-bearing arteries (Fig. 4b, d). Future integration with flexible mechanical sensors, such as an ultra-thin nitinol-based strain sensor[109], will provide it with tactile feedback, further enhancing the safety of movement within complex cerebrovascular anatomy. Zhang et al.[110] designed a magnetically actuated soft microcatheter that uses a soft silicone spiral tip and a ball joint to achieve dual-degree-of-freedom axial/radial rotation. In in-vitro tests on a human cerebral vascular model, it improved the efficiency of passing through an 80° S-shaped sharp bend analogous to the internal carotid artery, and reduced the transit time by over 20 s for vessels with acute-angle bifurcations and diameters smaller than 1 mm (similar to the MCA M3-M4 junction) (Fig. 4a). This microcatheter also has the ability to fragment and clear thrombi, and with optimized manufacturing processes, its diameter could potentially be reduced to less than 100 micrometers to meet the size requirements for peripheral artery embolism treatment (Fig. 4f).

However, the constraints of low-magnetic-field working environments limit the compatibility of most flexible magnetic navigation devices with MRI systems. Exploring integration with MRI will be a crucial development direction in this field.

Exploring integration with MRI will be a crucial development direction in this field. While certain MR-conditional catheters, such as EmeryGlide™[111] and EPflex[112], have been implemented in vascular interventions, they notably lack magnetic steering capabilities. The steering functionality of flexible magnetic navigation devices typically relies on the precise modulation of the direction, intensity, and gradient of an externally generated magnetic field. In contrast, MRI imaging is fundamentally predicated on a highly homogeneous and stable static magnetic field. This fundamental discrepancy constitutes the core conflict limiting their compatibility. The ferromagnetic materials employed in conventional magnetic navigation devices can severely perturb the homogeneity of the main magnetic field, resulting in significant image distortion[113]. Furthermore, the intrinsic magnetic fields generated by these devices may interfere with the MRI radiofrequency (RF) reception signals, thereby introducing image artifacts.

Despite Mehmet Efe Tiryaki et al.[114]. invented a magnetic guidewire suitable for 7 T ultra-high-field MRI (Fig. 4e). However, unlike the 1.5/3.0 T magnetic field strengths commonly used in clinical MRI, ultra-high fields, while offering advantages of high signal-to-noise ratio and high contrast, also face challenges such as RF field inhomogeneity and increased specific absorption ratio (SAR)[115]. The feasibility of using this for long-duration interventional guidance operations needs to be considered. Additionally, the magnetic material at the tip of the flexible guidewire and any metal implants in the patient's body can disturb the magnetic field environment, producing artifacts such as signal loss, geometric distortion, and edge blurring, which can distort the MRI image[116].

The opportunity to achieve the integration of magnetic navigation with MRI lies in the development of MRI-compatible magnetic functional materials. For instance, the novel Zr-Ru alloy developed by Li et al.[117] exhibits a low magnetic susceptibility ranging from 1.25×10^{-6} to 1.29×10^{-6} $cm^3 \cdot g^{-1}$, rendering it suitable for the MRI diagnostic environment. Additionally, it has demonstrated superior mechanical properties, corrosion resistance, and biocompatibility across a series of rigorous tests. A novel Zr-16Nb-xTi alloy developed by Xue et al.[118] has been shown to possess foreseeable MRI compatibility by virtue of its low magnetic susceptibility. It effectively overcomes the dilemma of traditional low-magnetic-susceptibility materials having a high Young's modulus, while also meeting requirements for a certain degree of flexibility, good biocompatibility, adequate corrosion resistance. Furthermore, the emerging permanent-fluidic-magnet-based liquid technology[119], through a three-dimensional directional branched magnetic network structure, has achieved precise control of the magnetic susceptibility within the order of 10^{-6}, providing a new approach for liquid materials for MRI-compatible magnetic navigation devices. Compared with traditional rigid materials, fluid magnets, due to their injectable and reconfigurable properties, can better adapt to the dynamic deformation of biological tissues, providing an innovative solution for matching the interface between magnetic navigation catheters and tissues. Collectively, these advancements provide a robust materials science foundation for the flexibilization of magnetic navigation and its compatibility with MRI systems. However, the miniaturization of low-magnetic-susceptibility materials may lead to a decrease in the magnetic response

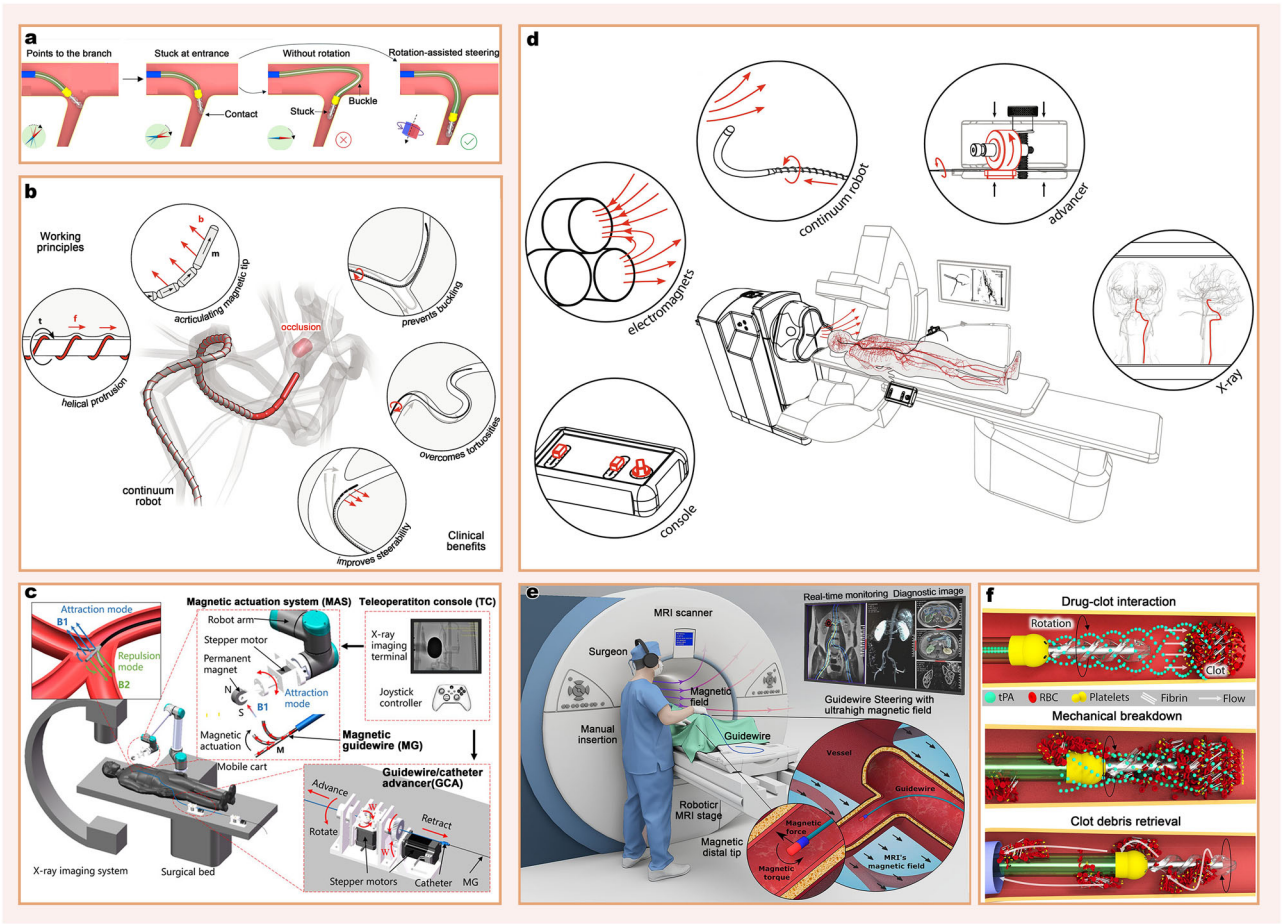


Fig. 4 | Flexible magnetic guidewires/catheters and surgical robot systems suitable for panvascular interventional therapy. a Optimized steering strategy of magnetically actuated soft rotatable-tipped microcatheter (MSRM) when dealing with sharp vascular branches. Reproduced with permission[110]. Copyright © 2025, The American Association for the Advancement of Science. **b** Working schematic of advancement and flexible steering of Helical magnetic continuum robot (mCR) with articulated magnetic tip. Reproduced with permission[108]. Copyright © 2024, The American Association for the Advancement of Science. **c** Conceptual diagram of clinical application of magnetically controlled guidewire robot system (MCGRS). Reproduced with permission[121]. Copyright © 2023, John Wiley and Sons. **d** Overview of the working mode of a surgical robot system based on Helical magnetic continuum robot. Reproduced with permission[108]. Copyright © 2024, The American Association for the Advancement of Science. **e** Interventional surgical robot system suitable for ultrahigh fields (UHF). Clinical scenario where a surgeon uses magnetic resonance imaging (MRI) guidance and the internal magnetic field of scanners to manipulate the magnetic guidewire. Reproduced with permission[114]. Copyright © 2023, The American Association for the Advancement of Science. **f** Working schematic of magnetically actuated soft rotatable-tipped microcatheter (MSRM) promoting drug-thrombus interaction, rotationally clearing, and retrieving thrombus fragments. Reproduced with permission[110]. Copyright © 2025, The American Association for the Advancement of Science.

performance of flexible guidewires/catheters[120], necessitating continued exploration of superior electromagnetic performance for MRI-compatible flexible magnetic navigation devices.

The synergistic paradigm of flexible magnetic navigation devices and surgical robot systems will reconstruct the logic of interventional guidance through the dual automation of steering and propulsion. For example, Fu et al.[121], focusing on automatic trajectory planning and motion control algorithms, designed a Magnetically Controlled Guidewire Robot System. Its magnetic actuation module uses a UR10 robotic arm to carry permanent magnets, generating a non-uniform magnetic field that uses magnetic torque to deflect the tip of the magnetic guidewire. It also incorporates a guidewire/catheter propulsion module consisting of a stepper motor with a friction wheel to support complex movements like advancement, retraction, and rotation (Fig. 4c). In experiments with a 3D-printed vascular phantom, they successfully achieved precise guidewire/catheter delivery using an integrated remote operation console and a DSA X-ray imaging module. This type of leader-follower surgical robot system[122] not only effectively solves the "non-colocation" problem for physicians but also injects momentum into the implementation and promotion of remote surgery[123]. We envision establishing a surgical robot system within the Assistance stage of the "4 A Tetrahedron System" that exhibits higher compatibility and is specifically optimized for panvascular interventional therapy. This necessitates a synergistic convergence of flexible electronics across both imaging and navigation domains. Ultrasound/photoacoustic imaging systems, underpinned by flexible ultrasonic transducer arrays, provide the surgical robotic ecosystem with real-time, continuous intravascular visualization capabilities. This ensures the dynamic tracking of the magnetic guidewire/catheter's kinematic behavior within the lumen and its interaction with the vessel wall, offering enriched vascular environmental data and enhanced safety monitoring conditions. Concurrently, magnetic navigation devices based on flexible magnetic guidewires/catheters serve as the actuation terminals of the system. They translate updated intraoperative imagery into adaptive trajectory planning and tracking, effectively executing the imaging system's guidance intent through precise and stable propulsion (Fig. 4).

In the future, more comprehensive, flexible magnetic navigation devices will continue to enhance surgical robot systems and develop their advantages in precise guidance for panvascular interventional therapy,

becoming one of the front-runners in the Assistance stage of the "4 A Tetrahedron System".

Within the "base" of the "4 A Tetrahedron System", the intraoperative procedures of the Assistance stage directly determine the success rate of panvascular surgery and are a vital link in safeguarding the patient's lifeline. Atherosclerosis is an important pathological feature of panvascular disease. Guided by ultrasound/photoacoustic imaging, the physician controls the advancement of a flexible magnetic guidewire/catheter using the robotic arm of a surgical system. During delivery, the motion algorithm of the guidewire tip senses and measures intraluminal data, such as the structure of the intimal surface, morphology of fibrous plaques and the morphology and size of the lumen, in real time. This data is used to reconstruct a 3D virtual vessel at the terminal, which corroborates the diagnostic results from the Assessment stage, provides feedback on any blind spots in preoperative testing, and allows for timely correction of initial judgments. It can also provide guiding suggestions for the selection of smart interventional devices in the Assessment stage. Characteristics such as thin fibrous caps, large lipid core volumes, and the presence of inflammatory cells make the rupture of unstable plaques a risk factor for sudden postoperative acute thrombosis. The imaging results from the Assistance stage will maximize the synchronization of vascular information. It not only directs the focus of postoperative follow-up in the Aftercare stage at the original lesion site, but also enables the examination of vessels along the intervention path through the automatic steering of the magnetic guidewire/catheter, contributing to a precise monitoring of the patient's recovery. This highlights the adaptability of the "4 A Tetrahedron System" to the systemic nature of panvascular disease affecting vascular beds throughout the body. This will greatly enhance the suitcordance between the "4 A Tetrahedron System"-a synergistic framework composed of flexible electronic devices-and the human body.

Aftercare: doctor-patient continuous telemonitoring & organ-crossed multiscale networks

Post-interventional management in panvascular disease faces multidimensional clinical challenges. The spatiotemporal heterogeneity of disease progression means that even after intervention in a single vascular bed, the atherosclerotic process continues in other areas[124,125]. The insidious nature of late complications makes it difficult to detect risks such as restenosis and in-stent thrombosis in a timely manner through traditional follow-up[126,127]. Furthermore, the absence of coordinated multi-organ monitoring hinders the holistic prevention and control of panvascular disease[1]. The current passive prognostic model, which relies on outpatient follow-ups and imaging studies, exposes numerous drawbacks, including discrete monitoring, fragmented data, and delayed warnings. The establishment of a comprehensive post-interventional management system for panvascular disease has shown significant clinical urgency. This necessitates the acceleration of the construction of IoMT-based "Medical Wireless Sensor Networks"[128] by flexible electronic devices to provide patients with round-the-clock, comprehensive monitoring, thereby establishing a new platform for the Aftercare stage of the "4 A Tetrahedron System".

This stage is critical for the continuous monitoring and maintenance of long-term suitcordance, detecting subtle deviations from biological concordance that could lead to adverse events.

The "Internet of Medical Things" (IoMT) can transmit clinical data collected by sensors to a remote cloud center for analysis via technologies like Bluetooth and Wi-Fi, serving as a powerful assistant for monitoring patient conditions and assessing disease progression[129]. "Doctor-patient connection" and "whole-body connection" are two key features of building "Medical Wireless Sensor Networks" in the context of IoMT. This framework not only emphasizes the synergistic effect of remote monitoring of patient vital signs and real-time alerts for physicians but also integrates the patient's own cross-organ, multi-scale flexible sensors to achieve systemic management of panvascular disease, highlighting the significant role of flexible electronic devices in the Aftercare stage of post-interventional therapy.

Distinct from the flexible sensors discussed in the Assessment stage, those employed in constructing "Medical Wireless Sensor Networks" prioritize performance and contributions toward addressing challenges of systemic integration. First, possessing stable wireless signal transmission capabilities is essential. Electromagnetic interference is frequently induced by other metallic components within the body. Furthermore, signal transmission from implantable sensors is susceptible to the adverse effects of dynamic internal environmental changes and tissue attenuation. The spatiotemporal resolution differences in the signal responses of flexible sensing devices working together lead to cascading calibration offsets. Consequently, flexible sensors operating within "Medical Wireless Sensor Networks" must maintain a low bit error rate and a high signal-to-noise ratio in communication to prevent the distortion of measured parameters. Second, the compatibility between flexible sensors and remote governing systems is emphasized. This necessitates the establishment of a unified architecture and database for the multi-modal data streams generated by diverse sensors.

Flexible sensors in "Medical Wireless Sensor Networks" are the prerequisite for perfecting the remote real-time warning mechanism in post-interventional care, thus achieving the "doctor-patient connection". For example, the disposable wireless patch sensor "VitalPatch", designed by Selvaraj et al.[130], integrates a system-on-chip (SoC) processor, onboard memory, and a Bluetooth Low Energy (BLE) transceiver to achieve real-time signal computation, wireless communication, and data transmission. Physicians can use the Vista Solution™ platform on a computer or tablet to remotely monitor the patient's heart rate, respiratory rate, skin temperature, and other vital signs to prevent acute cardiovascular events. It can also analyze the patient's body posture and movement status to prevent falls, playing a positive role in home health monitoring for the elderly. The smart insole system designed by Abbott et al.[131] consists of an insole with eight flexible pressure sensors distributed across the sole and a smartwatch for real-time monitoring. Through a pressure feedback system, a real-time pressure map of the sole is displayed on the smartwatch screen, which can promptly issue alarms to remind patients with diabetic foot to relieve plantar pressure, significantly reducing the risk of postoperative recurrence. Future "Medical Wireless Sensor Networks" will need to further optimize the remote real-time warning mechanism through two information feedback pathways-to both the doctor and the patient. This will help patients establish healthy lifestyle habits conducive to recovery and prevent postoperative complications of panvascular disease, while also providing physicians with a large volume of follow-up data to adjust personalized treatment strategies in a timely manner, thereby promoting the popularization of precision medicine.

A deployment model of flexible sensors that is cross-organ and multi-scale interactive is another driving force for deepening the connection between "Medical Wireless Sensor Networks" and the "Internet of Medical Things", and is the primary way to achieve the "whole-body connection." On one hand, flexible sensors for monitoring panvascular diseases related to organs like the heart[14,132–134] (Fig. 5b), brain[17,133,135–138] (Fig. 5a), kidneys[139,140], and limbs[18,141–143] (Fig. 5e) are already widely used, but mostly in isolation. A "Medical Wireless Sensor Network" that covers multiple organs is needed for comprehensive postoperative monitoring of patients to prevent disease progression and recurrence. On the other hand, the three types of flexible sensors-wearable[144–147] (Fig. 5c), semi-implantable[22,148–150] (Fig. 5d) and implantable[151–154] (Fig. 5f) —have functionally distinct roles due to their different depths of tissue invasion. Wearable sensors predominantly interface with the epidermis or superficial tissues, semi-implantable variants extend their operational reach to subcutaneous or mucosal layers, whereas implantable sensors are positioned directly adjacent to deep-seated tissues or organs. When these distinct sensor categories operate concurrently, the modalities, temporality, and spatial resolution of the acquired signals diverge significantly. Furthermore, variations in biological responses across different tissue interfaces, coupled with non-uniform signal transmission mechanisms, tend to fragment the coherence of multi-source data streams. This fragmentation can reduce diagnostic efficiency for physicians, as data from deep implantable sensors (e.g., vessel pressure) and surface wearable

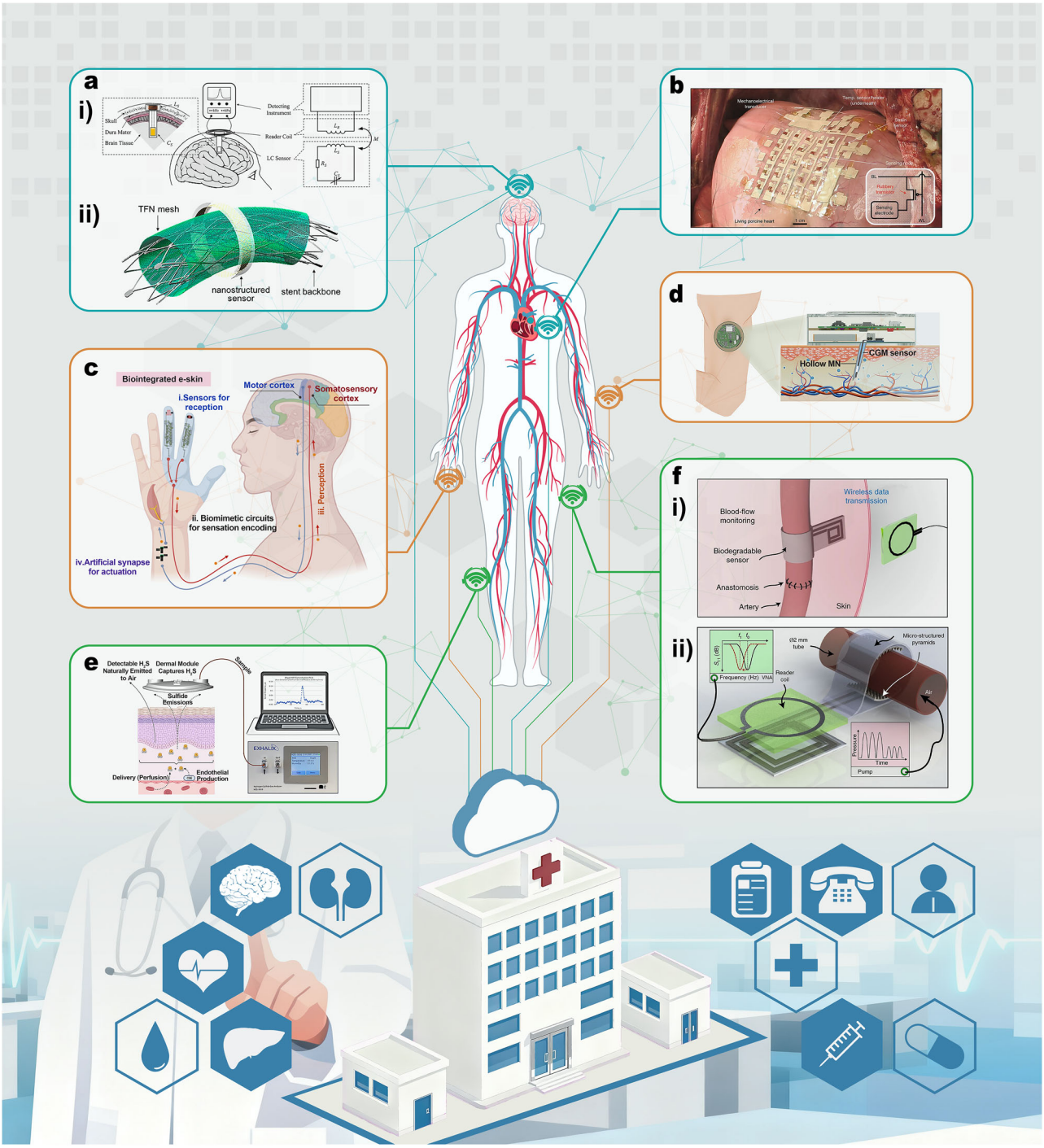


Fig. 5 | Conceptual diagram of "Medical Wireless Sensor Networks" with "doctor-patient" and "whole-body" connections. a (i) Schematic of the wireless passive intracranial pressure monitoring system. Reprinted with permission[137]. Copyright © 2019, Springer Nature. (ii) Overview of the integrated flow-diverter system. Hemodynamic changes in intracranial aneurysms can be detected via flow sensors. Reprinted with permission[138]. Copyright © 2018, American Chemical Society. **b** and physical photos of its components attached to a porcine heart, capable of spatio-temporal mapping of measurements such as electrophysiology, strain, and temperature. Reproduced with permission[134]. Copyright © 2020, Springer Nature. **c** Schematic diagram of the working principle of neuromorphic computing systems based on biointegrated e-skin for an artificial sensorimotor loop. Reproduced with permission[147]. Copyright © 2023, The American Association for the Advancement of Science. **d** Schematic diagram of a sensing system for Continuous glucose monitoring (CGM) via transdermal ISF glucose detection. Reproduced with permission[150]. Copyright © 2023, American Chemical Society. **e** Working principle schematic of Transdermal arterial gasotransmitter sensor (TAGS), detecting peripheral vascular endothelial function by collecting and measuring hydrogen sulfide concentration on the skin surface. Reprinted with permission[141]. Copyright © 2023, Elsevier. **f** (i) Working schematic of an implantable arterial pulse monitoring sensor. Data collected by the capacitive pulse sensor can be wirelessly transmitted through the skin. (ii) Schematic diagram of an in vitro experiment simulating facial arterial pulsation. Reproduced with permission[154]. Copyright © 2019, Springer Nature.

sensors (e.g., ECG) are often isolated in incompatible systems with mismatched timestamps, making it difficult to correlate them for a holistic diagnosis. For example, delayed or incomplete correlation between transient intravascular pressure spikes detected by implantable sensors and concurrent surface ECG abnormalities may obscure the early identification of restenosis-related ischemic events. This highlights the need for a "Medical Wireless Sensor Network" to centrally manage these multi-level sensors. A "Medical Wireless Sensor Network" that achieves a "whole-body connection" through cross-organ, multi-scale flexible sensors can overcome the shortcomings of traditional single-organ monitoring, where affected areas are easily missed. It allows for a comprehensive assessment that considers the systemic and whole-body nature of panvascular disease. It also leverages the respective advantages of wearable, semi-implantable, and implantable sensors, reflecting the macroscopic and microscopic connections of pathological states from different tissue depths of the body, and preventing inaccurate causal judgments from hindering emergency response.

The "whole-body connection" working model generates a systemic pathological map through multi-organ, multi-level flexible sensors, strengthening the spatiotemporal correlation of patient health monitoring data. This can effectively resolve the barrier of information asymmetry between doctors and patients, optimizing the accuracy and efficiency of the "doctor-patient connection". With the gradual increase in internet penetration, "Medical Wireless Sensor Networks" based on the dual features of "doctor-patient connection" and "whole-body connection" will significantly improve medical accessibility in remote or medically underserved areas, effectively alleviating the burden of social determinants of health and promoting the synergistic advancement of medical efficiency and health equity[155].

The journey to implementing "Medical Wireless Sensor Networks" with "doctor-patient" and "whole-body" connections is fraught with challenges, and its future exploration is equally arduous. Data security, the biggest concern in remote wireless data transmission, faces severe tests. Although Jabeen et al.[156] in 2023 attempted to construct a wireless intelligent healthcare system combined with IoMT, using complex genetic algorithms and lightweight cryptography to encrypt the data stream from the sensor to the transmission channel, and protecting it with a dual "device-user" ID authentication mechanism. In model testing, it successfully resisted four different types of cyberattacks, showing good application prospects. Beyond data security, limitations such as the low accessibility of core component flexible sensors, high maintenance costs for cloud servers, demanding network requirements for high bandwidth and low latency, and surging energy consumption also hinder the popularization of medical informatization[129,157]. Furthermore, the unresolved conflict between the high power consumption of implantable devices and the low efficiency of energy supply is also worthy of attention. Transcutaneous energy transmission methods such as near-field inductive coupling, far-field electromagnetic coupling, and ultrasonic energy transfer suffer from significant energy attenuation loss and low utilization when targeting deep vascular beds[158]. The power generation limitations of self-powering methods such as triboelectric nanogenerators (TENGs) and piezoelectric nanogenerators (PENGs)[159], along with the miniaturization requirements for energy storage units, make it challenging to support the continuous operation of an integrated sensor network. High energy density can also have toxic side effects on cells and tissues, potentially leading to long-term biocompatibility issues.

Within the "base" of the "4 A Tetrahedron System", the comprehensive postoperative follow-up of the Aftercare stage is an effective means of improving the prognosis of panvascular interventional therapy and reducing the rates of disease recurrence and complications. Thanks to the "doctor-patient connection" and "whole-body connection" features of the "Medical Wireless Sensor Network", physicians can remotely interface with patients through flexible health monitoring devices. This input loops back into the Assessment stage, guiding the design of interventional device parameters and functional improvements. It utilizes real-world clinical cases as a foundation to identify directions for optimization and further research. The patient's follow-up database can also provide a referable and predictable standard for the often-ambiguous empirical aspects of the intraoperative Assistance stage. The "Medical Wireless Sensor Network" offers a long-term vision for post-interventional monitoring in panvascular therapy. Flexible electronic devices support the Aftercare stage in achieving doctor-patient continuous telemonitoring and constructing an organ-crossed multiscale network, holding a pivotal strategic position in the establishment of the triangular circulation of the "base" of the "4 A Tetrahedron System".

AI-retrofit: algorithm-driven capability augmentation & multi-sourced dataflow integration

In the era of rapid artificial intelligence development, the application of AI in the medical field has become a hot topic, playing a significant role in areas such as image analysis, clinical diagnosis, and rehabilitation care[160–162]. As the pinnacle of the "4 A Tetrahedron System", the AI-retrofit stage refer to the algorithm-driven enhancement of capabilities and integration of multi-sourced dataflows. This stage will further strengthen the role of AI in comprehensive perioperative management, with the ultimate objective of making the system dynamic. This involves not only optimizing the performance of flexible electronic devices throughout the preoperative, intraoperative, and postoperative processes from a technical and equipment perspective-achieving a synergistic improvement in work efficiency and patient experience-but also coordinating the planning of the first three "A"s (Assessment, Assistance, and Aftercare) at a global level. By leveraging massive clinical data, AI strengthens the organic connections and feedback loops among the four stages. The transmission and flow of data, guided by AI algorithms, will become the engine for the "4 stages-6 routes-12 relationships" within the "4 A Tetrahedron System".

In the Assessment, Assistance, and Aftercare stages, the optimization effects on flexible electronic devices empowered by AI are already taking shape, and the connection between the "apex" and the "base" of the "4 A Tetrahedron System" is becoming increasingly close.

In Assessment, AI has demonstrated strong vitality in areas such as process prediction, material research and development, and design optimization. Rezapour et al.[163] designed an AI framework combining deep learning and machine learning for the quality inspection and process prediction of 3D-printed degradable microneedle arrays. Initially, a deep learning model was developed to classify products from imaging data, identifying defective microneedle arrays. Model performance was evaluated via a confusion matrix, focusing on the false positive rate to guide iterative optimization. They then trained a machine learning model to enable users to seamlessly predict product performance under different parameters and processes, significantly improving the production efficiency and quality of microneedle arrays. In the future, the organic integration of AI with materials informatics will also continue to focus on the discovery, construction, and optimization of material structures, aiding in the performance enhancement of flexible microneedle platforms[164]. A prominent example is the Crystalyze framework developed by Riesel et al.[165], a generative machine learning model that uses convolutional neural networks and multi-layer perceptrons to analyze powder X-ray diffraction patterns. It can generate and predict crystal structures without any experimental models, significantly accelerating material discovery and research, and holding promise for solving the promotion challenges of flexible microneedle platforms in the Assessment stage. Furthermore, Hachem et al.[166] developed a model targeting the personalized design of flow-diverter stents for patients with intracranial aneurysms. They coupled multi-physics computational fluid dynamics (CFD) and deep reinforcement learning (DRL) to optimize the non-uniform porosity distribution. Leveraging 3D vascular geometries and hemodynamic data from two patients, the model achieved a significant reduction in post-stenting wall shear stress and inflow velocity at the aneurysm neck. In the future, AI is poised to permeate the entire lifecycle of flexible microneedle platforms and smart interventional devices, spanning from conceptualization to clinical application. It will be specifically integrated into the Assessment stage of the "4 A Tetrahedron System," aiming to enhance the "suitcordance" of panvascular interventional devices empowered by flexible electronics.

Table 1 | The core functions of AI-retrofit stage in the "4 A Tetrahedron System"

Core Functions (AI-Retrofit)	Key AI Technology/Model	Data Source (Data Influx)	Retrofit Output (Optimization Output)	Optimization Goal (Target)
Full-Cycle Data Integration & Closed-Loop Feedback	Reinforcement Learning (RL), Knowledge Graph	Assessment: ISF Biomarkers, Device Design Data Assistance: Intraoperative Imaging, Guidewire Movement Data Aftercare: Remote Monitoring Data, Prognostic Trends	Comprehensive Clinical Decision Support System (CDSS)	Connecting Data Silos across Stages Achieving Dynamic Interactivity
Device Performance Iteration & Optimization	Deep Learning (DL), Materials Informatics (MI)	Assessment: Microneedle Array Quality Inspection Images Aftercare: Smart Stent Continuous Strain Data, Postoperative Restenosis/Thrombus Signals	Assessment: Optimization suggestions for next-generation smart device Geometric Configuration and Material Composition; Microneedle Production Parameter Prediction	Enhancing Device Suitcordance (Short-term Suitability and Long-term Harmony)
Intraoperative Intelligent Guidance & Automation	FCN-32 Deep Learning Network, MSAC Algorithm, VGG13 Model	Assessment: Preoperative CT/MRI Images, Vascular Anatomy Data Aftercare: Comparison of Magnetic Navigation Decisions and Vascular Prognosis	Assistance: Magnetic Navigation Trajectory Planning, Real-time Tracking, Magnetic Field Strength Adjustment; Ultrasound Imaging Automatic Positioning	Increasing the Automation Level Precision and Safety of Interventional Procedures
Remote Monitoring & Warning Accuracy Improvement	Hybrid Core Architecture (CNN + LSTM), Artificial Neural Network (ANN)	Aftercare: Multi-source Flexible Sensor Data (Blood Pressure, Heart Rate, Blood Oxygen); Static Patient Information (Age, Medical History)	Aftercare: Setting Abnormal Thresholds for Remote Monitoring; Continuous improvement in Real-time Warning mechanism Accuracy	Achieving Precision Medicine and Remote Healthcare Accessibility

Crucially, beyond device optimization, AI algorithms directly empower clinical assessment by analyzing longitudinal trends in ISF biomarkers to predict disease progression risks, thereby transforming raw sensing data into actionable diagnostic insights. AI models trained on large-scale interstitial fluid (ISF) biomarker datasets—integrated with imaging, physiological, and demographic data—enable advanced biomarker interpretation, patient phenotyping, and dynamic risk stratification. Such data-driven approaches allow the early identification of pathological deviations that may not be evident from single biomarkers or static thresholds alone[167,168]. For example, machine learning–based models can uncover latent patterns across multi-analyte ISF profiles to predict restenosis risk, inflammatory burden, or vascular instability prior to intervention, thereby informing personalized procedural planning and device selection. In this context, AI functions not merely as a downstream analytical tool, but as a core component of the Assessment stage, closing the loop between biological sensing, clinical decision-making, and precision panvascular intervention.

In Assistance, Hu et al.[84] trained an FCN-32 deep learning neural network to predict left ventricular volume waveforms, cardiac output, and ejection fraction from B-mode ultrasound images acquired by a flexible ultrasound patch. Yang et al.[169] designed a surgical robot system that uses the M-estimator sample consensus (MSAC) algorithm to fit a polynomial for planning the trajectory of a magnetic guidewire. The 3D point cloud and centerline data extracted during the process can be registered with other preoperative information to adjust model parameters. Combined with normalized cross-correlation (NCC) for real-time tracking of the magnetic guidewire, it can also change the magnetic field strength based on the path curvature, enhancing the automation level of interventional guidance. The previously mentioned USoP[80] already uses a VGG13 machine learning model for continuous tracking and positioning of moving target vessels, highlighting the crucial role of AI in "fully autonomous" flexible electronic devices for panvascular interventional therapy. For example, in neuromorphic computing systems, the integration of computation and storage units, along with the coupling of sensing and analysis modules, will eliminate the dependence on external devices, thereby saving significant energy loss due to data transmission[170]. Reconfigurable neuromorphic computing technology, derived from this basis, can integrate more personalized neuromorphic computing paradigms in a unified manner, maximizing the use of limited hardware resources through reallocation to perform complex, repeatable brain-like functions[171]. With continuously increasing integration, flexible electronic devices will exhibit even broader application scenarios in the Assistance stage of panvascular interventional therapy.

In Aftercare, the application scenarios of AI deep learning algorithms in the Internet of Medical Things (IoMT) are being widely explored. Najim et al.[172] designed a deep learning-based health monitoring system by inputting multi-source flexible sensor data and static patient information (age, medical history, etc.) into an artificial neural network (ANN). It can monitor basic parameters such as blood pressure, heart rate, blood oxygen levels, and body temperature in real time with an accuracy of up to 98.7% and upload the data to the cloud. Physicians can intuitively obtain long-term trends of patient data and set up an automatic alert mechanism for dangerous thresholds. The integration of a 5 G network further enables applications and deployments in remote regions. Alharbe et al.[173] developed a hybrid core architecture combining Convolutional Neural Networks (CNNs) and Long Short-Term Memory (LSTM) units. In addition to the basic functions of arrhythmia classification and disease risk prediction, it uses blockchain technology for encryption to ensure data security. The powerful computational capabilities of deep learning algorithms provide a reliable tool for monitoring abnormal vital signs in patients, and the unique and complex data encryption techniques offer a guarantee for preventing information leakage and improving the security of remote data transmission. In the future, IoMT-based "Medical Wireless Sensor Networks" will also leverage the self-learning capabilities of artificial intelligence to continuously improve the accuracy of remote warnings, providing technological support for the Aftercare stage (Table 1).

Beyond the predictive capabilities of traditional supervised learning, Deep Reinforcement Learning (DRL) has emerged as a pivotal paradigm for optimizing comprehensive clinical decision support systems (CDSS)[174]. Liu et al.[175] constructed an intelligent ranking system based on an actor-critic architecture via the Proximal Policy Optimization (PPO) algorithm. Its Actor network, inspired by the deep & cross network, modeled the intricate relationships between high-dimensional cell lines and drug features to generate personalized drug ranking probability distributions for each patient. Meanwhile, the Critic network assessed the value of the policies proposed by the Actor network. Utilizing normalized discounted cumulative gain (NDCG) as the reward signal, the system achieved continuous policy iteration through the PPO algorithm. Experimental results demonstrated that its performance on two real-world datasets—the Genomics of Drug Sensitivity in Cancer (GDSC) and the Cancer Genome Atlas (TCGA)—significantly surpassed traditional supervised learning methods. This validates the dynamic updating and continuous learning capabilities of DRL approaches within CDSS contexts.

Niraula, D. et al.[176] developed an Adaptive Radiotherapy Clinical Decision Support (ARCliDS) framework composed of an Artificial RT Environment (ARTE) and an Optimal Decision Maker (ODM). Its utilization of Double Graph Neural Networks significantly mitigated the influence of non-physical factors when processing inter-feature relationships. Subsequently, a Wasserstein Generative Adversarial Network with Gradient Penalty (WGAN-GP) was trained to augment clinical data for the ODM and facilitate dynamic optimization. Ultimately, in clinical trials involving adaptive stereotactic body radiotherapy (SBRT) for patients with non-small cell lung cancer (NSCLC) and hepatocellular carcinoma (HCC), the system reproduced 36% and 50% of superior clinical decisions, respectively, while improving upon 74% and 30% of suboptimal decisions. Including the aforementioned examples, the application of DRL in cancer CDSS—primarily manifested in medication dosage adjustment and radiotherapy strategy optimization[177,178]—offers a valuable reference trajectory for the prognosis management of panvascular interventions. In the context of the "4 A Tetrahedron System", managing panvascular disease is fundamentally a sequential decision-making problem where optimal actions (e.g., medication dosage, timing of re-intervention) depend on the evolving physiological state of the patient. DRL algorithms, such as Deep Q-Networks (DQN) or Proximal Policy Optimization (PPO), can function as intelligent agents that interact with the continuous data streams provided by flexible sensors in the Aftercare stage. By treating patient health improvements as "reward signals" and sensor readings as "state observations", DRL models can frame the Aftercare stage as a Markov Decision Process to learn to formulate personalized Dynamic Treatment Regimes (DTRs). For instance, an RL-based agent could analyze long-term blood pressure variability and vessel wall stress data to recommend adaptive antiplatelet therapy dosages, thereby maximizing therapeutic efficacy while minimizing bleeding risks over time. This shifts the AI-retrofit stage from static risk prediction to dynamic, long-term strategy optimization.

Furthermore, the advent of Large Language Models (LLMs) and Multimodal Large Language Models (MLLMs) offers unprecedented potential to enhance the interpretability and interactivity of the "4 A Tetrahedron System". The vast amount of heterogeneous data generated across the Assessment (molecular biomarkers), Assistance (surgical imaging), and Aftercare (wearable time-series signals) stages often creates an information bottleneck for both clinicians and patients. LLMs can serve as a cognitive interface to synthesize these multi-source dataflows. By leveraging advances in natural language processing and knowledge graph integration, LLMs can automatically generate comprehensive, human-readable clinical reports that contextualize complex sensor data against the latest medical literature. For instance, Lavender Yao Jiang et al.[179] introduced a health system-scale large language model termed NYUTron. It utilized unstructured clinical notes extracted from the electronic health records (EHRs) of over 387,000 patients as a pre-training corpus. Employing a BERT architecture, the study trained a 109-million-parameter multi-task clinical prediction engine. This model not only exhibited robust performance across five prediction tasks—30-day readmission, in-hospital mortality, comorbidity index, length of stay, and insurance denial—but also achieved an Area Under the Curve (AUC) improvement ranging from 5.36% to 14.7% over traditional models. Furthermore, it marked the first clinical deployment of such a large language model, underscoring the substantial value of LLMs in the Aftercare stage. Moreover, LLM-powered conversational assistants can transform the patient experience in the Aftercare stage; instead of viewing raw data logs, patients can interact with a "virtual health consultant" to understand the implications of their physiological fluctuations in real-time. This integration not only democratizes access to complex medical insights but also facilitates a more intuitive, logic-driven feedback loop within the AI-retrofit framework (Table 2).

As the "apex" of the "4 A Tetrahedron System", the AI-retrofit stage also emphasizes the flexible transmission and cross-utilization of data flows. Its innovation in panvascular interventional therapy lies in using flexible electronic devices to build a bridge for the flow of patient clinical data throughout the entire process. This enriches and updates the content of the training and validation sets for device models at each stage, driving model iteration and optimization. For example, the implantable sensor of a coronary smart stent (Aftercare) acquires a continuous stream of strain data after panvascular intervention. On one hand, this data is fed into a stent production machine learning model (AI-retrofit). After being trained on massive follow-up data, the model's ability to identify and predict the characteristic signals of abnormal neointimal hyperplasia is enhanced, which then guides the optimization of the geometric configuration of the next generation of smart stents (Assessment) to improve vessel wall apposition and reduce shear stress. On the other hand, the data is input into the surgical robot system's deep learning model (AI-retrofit). This study analyzes and compares the effects of steering decisions made by magnetic navigation devices on vascular prognosis, thereby refining interventional guidance strategies tailored to diverse vascular environments. The cascading effect of the data flow across the four stages-Assessment, Assistance, Aftercare, and AI-retrofit-constructs the six bidirectional routes of the "4 A Tetrahedron System", forming a complex network of 12 relationships. During the AI-retrofit stage, the seamless integration of flexible electronic devices and artificial intelligence enhances the algorithm-driven capabilities of interventional devices and enables multi-source data flow integration, driving a paradigm shift in the preoperative, intraoperative, and postoperative phases- from operating independently to becoming dynamically interactive.

Summary and future directions

The "4 A Tetrahedron System", through the extensive and deep participation of flexible electronic devices, establishes a four-element synergistic architecture with "Assessment-Assistance-Aftercare-AI-retrofit" as its core thread, achieving a paradigm shift in the entire process of panvascular interventional therapy.

The Assessment stage utilizes flexible sensing devices to quantitatively analyze key parameters of the patient's condition while synchronously refining the evaluation system for device "suitcordance", and dynamically optimizing interventional device design. The Assistance stage requires flexible electronic devices achieve dual breakthroughs in imaging capabilities and operational performance during interventional guidance to improve surgical efficiency and safety. The Aftercare stage necessitates the establishment of "Medical Wireless Sensor Networks", where multi-organ and multi-level flexible health monitoring devices enable real-time postoperative monitoring and remote warnings through "doctor-patient connection" and "whole-body connection" methods. The AI-retrofit stage leverages artificial intelligence algorithms to eliminate data silos among the preoperative, intraoperative, and postoperative phases. It connects the flexible electronic devices of the first three stages to establish a closed-loop data feedback system.

The four stages are dynamically interconnected, making the "4 A Tetrahedron System" an innovative framework for future panvascular interventional therapy from the perspective of flexible electronics, providing

Table 2 | The Application Scenario of AI-retrofit stage in the "4 A Tetrahedron System"

Application Scenario	Function / Clinical Task	Key AI Technology / Model	Data Source	Optimization Target
Comprehensive Clinical Decision Support	Dynamic Treatment Regimen (DTR) Adaptive scheduling & dosage optimization	Deep Reinforcement Learning (DRL) (e.g., DQN, PPO, Actor-Critic)	Longitudinal sensor streams Electronic Health Records (EHR)	Maximizing long-term patient outcomes (reward) while minimizing adverse events
Intelligent Interaction & Synthesis	Multimodal Report Generation& Patient Consulting Synthesizing data into narrative insights	Large Language Models (LLMs) (e.g., Transformer-based architectures, Multimodal RAG)	Unstructured clinical notes Imaging data Sensor logs Guidelines	Enhancing data interpretability streamlining doctor-patient communication

a full-process reference solution for systematically addressing the challenges of panvascular disease.

However, the challenges that the "4 A Tetrahedron System" faces in its transition from a theoretical framework to clinical application are also worthy of attention.

Regulatory oversight and approval from relevant authorities are key to a product's transition from laboratory validation to clinical application. Strengthening the rigor of production processes to ensure product safety, efficacy, and quality control must be aligned with FDA/CE/NMPA standards, thereby accelerating to clinical translation. When facing the long approval times for FDA Class III medical devices, demonstrating substantial equivalence to existing medical devices can be a strategy to gain market access at a lower classification (Class II or Class I), which means that optimizing and improving existing designs may be more suitable for accelerating regulatory approval than creating entirely new ones[180]. Additionally, because the "4 A Tetrahedron System" aims to establish a highly integrated intelligent device system, the approval process for assessing the risk of combined failures and the extended period for algorithm validation may be more complex than for a single device. This requires the simultaneous updating and refinement of regulatory frameworks and industry standards to evaluate the safety and effectiveness of system-level medical products.

Furthermore, unhealthy lifestyle habits have become significant contributors to vascular diseases including hypertension and atherosclerosis. The trend of panvascular disease affecting younger people is becoming increasingly apparent, which highlights the vast patient base for panvascular disease and reflects the broad market prospects for interventional therapy and flexible electronic devices. Establishing a comprehensive industrial ecosystem that integrates "supply-manufacturing-distribution" is essential for advancing the convergence of flexible electronics with interventional devices and for addressing pressing clinical needs. With capital as the link, enterprises as the executive bodies, and business models as the accelerators, the pain points of insufficient promotion and low penetration of flexible electronic devices can be overcome. At the same time, government support needs to be strengthened by establishing large-scale, standardized industrial parks to actively guide cooperation in the R&D sector. Innovative and open incubation platforms should be established to foster collaboration among diverse innovation stakeholders, including enterprises, universities, research institutes, and medical institutions. Favorable funding policies for early-stage R&D investment should be implemented to effectively address the objective difficulties in establishing interdisciplinary platforms. It also calls for a three-way collaboration among material scientists, electronic information engineers, and clinical experts to break down disciplinary barriers and build an interdisciplinary collaborative innovation platform by leveraging the complementary advantages of materials science, electronic engineering, and biomedical and clinical medicine to overcome these hurdles.

In the next 10 years (2025–2035), the integration of flexible electronic devices and panvascular interventional therapy should follow the main thread of "Technology Breakthrough - Clinical Translation - Ecosystem Maturation". Advancement should proceed concurrently along three dimensions: interdisciplinary collaboration, regulatory adaptation, and industrial synergy.

During the Technology Breakthrough period (2025–2028), efforts will concentrate on overcoming key technical challenges and optimizing technical details.

The Clinical Translation period (2029–2032) should promote Phase III clinical trials and global product registration, and establish a standardized application system.

During the ecosystem maturation period (2033–2035), the development paradigm characterized by 'industry leadership and startup-driven innovation' is expected to be consolidated, thereby advancing the global integration of the industry.

Ultimately, the goal is to construct a panvascular interventional medical ecosystem from the perspective of flexible electronics, integrating medicine, engineering, and information technology, and fusing industry, academia, and research.

Data availability

No datasets were generated or analysed during the current study.

Received: 25 November 2025; Accepted: 19 January 2026;
Published online: 29 January 2026

References

1. Zhou, X., Yu, L., Zhao, Y. & Ge, J. Panvascular medicine: an emerging discipline focusing on atherosclerotic diseases. *Eur. Heart J.* **43**, 4528–4531 (2022).
2. GBD 2021 Diseases and Injuries Collaborators Global incidence, prevalence, years lived with disability (YLDs), disability-adjusted life-years (DALYs), and healthy life expectancy (HALE) for 371 diseases and injuries in 204 countries and territories and 811 subnational locations, 1990-2021: a systematic analysis for the Global Burden of Disease Study 2021. *Lancet* **403**, 2133–2161 (2024).
3. Guo, W. & Yi, X. Advancements and future prospects in the study of panvascular disease. *Clin. Hemorheol. Microcirc.* **89**, 198–204 (2025).
4. Chowdhury, M. & Secemsky, E. A. Atherectomy vs other modalities for treatment during peripheral vascular intervention. *Curr. Cardiol. Rep.* **24**, 869–877 (2022).
5. Schartz, D. et al. Impact of aspiration catheter size on clinical outcomes in aspiration thrombectomy. *J. Neurointerv. Surg.* **15**, e111–e116 (2023).
6. You, L., Luo, Y., Cheng, Q., Shen, L. & Ge, J. High-suitcordance intelligent fibers for panvascular disease monitoring-intervention. *Adv. Fiber Mater.* **7**, 1042–1072 (2025).
7. Yin, Z. et al. Inkjet printing for flexible electronics: materials, processes and equipments. *Chin. Sci. Bull.* **55**, 3383–3407 (2010).
8. Rogers, J. A., Someya, T. & Huang, Y. Materials and mechanics for stretchable electronics. *Science* **327**, 1603–1607 (2010).
9. Song, J. K. et al. Stretchable colour-sensitive quantum dot nanocomposites for shape-tunable multiplexed phototransistor arrays. *Nat. Nanotechnol.* **17**, 849–856 (2022).
10. Lee, S. et al. A shape-morphing cortex-adhesive sensor for closed-loop transcranial ultrasound neurostimulation. *Nat. Electron.* **7**, 800–814 (2024).
11. Jang, J. et al. Reconfigurable assembly of self-healing stretchable transistors and circuits for integrated systems. *Nat. Electron*. **8**, 474–484 (2025).
12. Jung, H. et al. Hydrogel–elastomer-based conductive nanomembranes for soft bioelectronics. *Nat. Nanotechnol.* **20**, 1822–1830 (2025).
13. Veletić, M. et al. Implants with sensing capabilities. *Chem. Rev.* **122**, 16329–16363 (2022).
14. Gao, W., Ota, H., Kiriya, D., Takei, K. & Javey, A. Flexible electronics toward wearable sensing. *Acc. Chem. Res.* **52**, 523–533 (2019).
15. Chen, S. et al. Flexible wearable sensors for cardiovascular health monitoring. *Adv. Healthc. Mater.* **10**, 2100116 (2021).
16. Kwon, K. et al. A battery-less wireless implant for the continuous monitoring of vascular pressure, flow rate and temperature. *Nat. Biomed. Eng.* **7**, 1215–1228 (2023).
17. Tang, H. et al. Injectable ultrasonic sensor for wireless monitoring of intracranial signals. *Nature* **630**, 84–90 (2024).
18. Wang, L. et al. Tracking peripheral artery motion and vascular resistance with a multimodal wearable sensor under pressure perturbations. *J. Biomech. Eng.* **144**, 081003 (2022).
19. Haghi, M., Thurow, K. & Stoll, R. Wearable devices in medical internet of things: scientific research and commercially available devices. *Healthc. Inform. Res.* **23**, 4–15 (2017).
20. Gubala, V., Harris, L. F., Ricco, A. J., Tan, M. X. & Williams, D. E. Point of care diagnostics: status and future. *Anal. Chem.* **84**, 487–515 (2012).
21. Rahmani, S. et al. 3D-printed microneedles in biomedical applications. *iScience* **24**, 102012 (2020).
22. Vora, L. K. et al. Microneedle-based biosensing. *Nat. Rev. Bioeng.* **2**, 64–81 (2024).
23. Hu, Y., Chatzilakou, E., Pan, Z., Traverso, G. & Yetisen, A. K. Microneedle sensors for point-of-care diagnostics. *Adv. Sci. (Weinh.)* **11**, e2306560 (2024).
24. Friedel, M. et al. Opportunities and challenges in the diagnostic utility of dermal interstitial fluid. *Nat. Biomed. Eng.* **7**, 1541–1555 (2023).
25. Xu, J., Yang, B., Kong, J., Zhang, Y. & Fang, X. Real-time monitoring and early warning of a cytokine storm in vivo using a wearable noninvasive skin microneedle patch. *Adv. Healthc. Mater.* **12**, e2203133 (2023).
26. Zheng, L., Zhu, D., Xiao, Y., Zheng, X. & Chen, P. Microneedle coupled epidermal sensor for multiplexed electrochemical detection of kidney disease biomarkers. *Biosens. Bioelectron.* **237**, 115506 (2023). 2023.
27. Huang, X. et al. 3D-assembled microneedle ion sensor-based wearable system for the transdermal monitoring of physiological ion fluctuations. *Microsyst. Nanoeng.* **9**, 25 (2023).
28. Ju, J., Li, L., Regmi, S., Zhang, X. & Tang, S. Microneedle-based glucose sensor platform: from vitro to wearable point-of-care testing systems. *Biosensors. (Basel)* **12**, 606 (2022).
29. Rawson, T. M. et al. Microneedle biosensors for real-time, minimally invasive drug monitoring of phenoxymethylpenicillin: a first-in-human evaluation in healthy volunteers. *Lancet Digit.al Health* **1**, e335–e343 (2019).
30. Li, Z. et al. Electrochemical detection of cholesterol in human biofluid using microneedle sensor. *J. Mater. Chem. B* **11**, 6075–6081 (2023).
31. Dervisevic, M. et al. Wearable microneedle array-based sensor for transdermal monitoring of pH levels in interstitial fluid. *Biosens. Bioelectron.* **222**, 114955 (2023).
32. Li, J. et al. Interstitial fluid biomarkers' minimally invasive monitoring using microneedle sensor arrays. *Anal. Chem.* **94**, 968–974 (2022).
33. Puttaswamy, S. V. et al. Nanophotonic-carbohydrate lab-on-a-microneedle for rapid detection of human cystatin C in finger-prick blood. *ACS Nano* **14**, 11939–11949 (2020).
34. Yang, J. et al. Microneedle-based integrated pharmacokinetic and pharmacodynamic evaluation platform for personalized medicine. *Nat. Commun.* **16**, 6260 (2025).
35. Ranamukhaarachchi, S. A. et al. Integrated hollow microneedle-optofluidic biosensor for therapeutic drug monitoring in sub-nanoliter volumes. *Sci. Rep.* **6**, 29075 (2016).
36. Zhu, J., Zhou, X., Libanori, A. & Sun, W. Microneedle-based bioassays. *Nanoscale Adv.* **2**, 4295–4304 (2020).
37. Yang, K. et al. A wearable dual-modal patch for rapid pre-hospital diagnosis of acute myocardial infarction. *ACS Nano* **19**, 23969–23981 (2025).
38. Chang, A. et al. Integration of chemical and physical inputs for monitoring metabolites and cardiac signals in diabetes. *Nat. Biomed. Eng.* **10**, 94–109 (2026).
39. Kutys, M. L. & Chen, C. S. Forces and mechanotransduction in 3D vascular biology. *Curr. Opin. Cell Biol.* **42**, 73–79 (2016).
40. Trimm, E. & Red-Horse, K. Vascular endothelial cell development and diversity. *Nat. Rev. Cardiol.* **20**, 197–210 (2023).
41. Shi, J., Yang, Y., Cheng, A., Xu, G. & He, F. Metabolism of vascular smooth muscle cells in vascular diseases. *Am. J. Physiol. Heart Circ. Physiol.* **319**, H613–H631 (2020).
42. Wei, K., Nguyen, H. N. & Brenner, M. B. Fibroblast pathology in inflammatory diseases. *J. Clin. Invest.* **131**, e149538 (2021).
43. Chistiakov, D. A. et al. Mechanisms of foam cell formation in atherosclerosis. *J. Mol. Med. (Berl.)* **95**, 1153–1165 (2017).
44. Lee, M. S. & Banka, G. In-stent restenosis. *Interv. Cardiol. Clin.* **5**, 211–220 (2016).

45. Mauri, L. et al. Relationship of late loss in lumen diameter to coronary restenosis in sirolimus-eluting stents. *Circulation* **111**, 321–327 (2005).
46. Chen, X., Assadsangabi, B., Hsiang, Y. & Takahata, K. Enabling angioplasty-ready "smart" stents to detect in-stent restenosis and occlusion. *Adv. Sci. (Weinh.)* **5**, 1700560 (2018).
47. Rigo, B. et al. Soft implantable printed bioelectronic system for wireless continuous monitoring of restenosis. *Biosens. Bioelectron.* **241**, 115650 (2023).
48. Hoare, D. et al. Predicting cardiovascular stent complications using self-reporting biosensors for noninvasive detection of disease. *Adv. Sci.* **9**, 2105285 (2022).
49. You, L., Shen, L. & Ge J. The foundation and development of China's National Basic Science Center for panvascular interventional complex systems: pioneering device-vessel suitcordance research. *Eur. Heart J*. **46**, 3400-3403 (2025).
50. Wang, L. et al. Ultra-sensitive wireless pressure sensor for real-time cardiovascular restenosis monitoring in smart stents. *IEEE 38th Int. Conf. Micro Electro Mech. Syst. (MEMS)*, 12–15 (2025).
51. Xu, H. et al. Flexible tensile strain-pressure sensor with an off-axis deformation-insensitivity. *Nano. Energy* **99**, 107384 (2022).
52. Sun, M. et al. Flexible graphene field-effect transistors and their application in flexible biomedical sensing. *Nano-Micro Lett.* **17**, 34 (2025).
53. Wang, L., Jackman, J. A., Ng, W. B. & Cho, N.-J. Flexible, graphene-coated biocomposite for highly sensitive, real-time molecular detection. *Adv. Funct. Mater.* **26**, 8623–8630 (2016).
54. Gao, J. et al. Ultrasensitive label-free MiRNA sensing based on a flexible graphene field-effect transistor without functionalization. *ACS Appl. Electron. Mater.* **2**, 1090–1098 (2020).
55. Hao, Z. et al. Measurement of cytokine biomarkers using an aptamer-based affinity graphene nanosensor on a flexible substrate toward wearable applications. *Nanoscale* **10**, 21681–21688 (2018).
56. Chen, L. et al. A DNA-functionalized graphene field-effect transistor for quantitation of vascular endothelial growth factor. *Sens. Actuators B.* **351**, 130964 (2022).
57. Ashraf, J. et al. Conducting Polymer-Infused Electrospun Fibre Mat Modified by POEGMA Brushes as Antifouling Biointerface. *Biosensors (Basel.)* **12**, 1143 (2022).
58. Zhang, S., Liu, W., Wu, Z. & Chen, H. Tri-functional platform for the facile construction of dual-functional surfaces via a one-pot strategy. *Mater. Chem. B.* **8**, 5602–5605 (2020).
59. Sheng, D. et al. Phosphorylcholine/heparin composite coatings on artificial lung membrane for enhanced hemo-compatibility. *Langmuir* **39**, 9796–9807 (2023).
60. Zhang, Z., Chen, S., Chang, Y. & Jiang, S. Surface grafted sulfobetaine polymers via atom transfer radical polymerization as superlow fouling coatings. *Phys. Chem. B.* **110**, 10799–10804 (2006).
61. Wu, Y. et al. 5 years of serial intravascular imaging outcomes of XINSORB sirolimus-eluting bioresorbable vascular scaffold. *JACC Cardiovasc. Interv.* **12**, 602–603 (2019).
62. Ouyang, H. et al. A bioresorbable dynamic pressure sensor for cardiovascular postoperative care. *Adv. Mater.* **33**, e2102302 (2021).
63. Chen, X. & Ahn, J. H. Biodegradable and bioabsorbable sensors based on two-dimensional materials. *J. Mater. Chem. B* **8**, 1082–1092 (2020).
64. Sun, Z. Synchrotron radiation computed tomography assessment of calcified plaques and coronary stenosis with different slice thicknesses and beam energies on 3D printed coronary models. *Quant. imaging Med. Surg.* **9**, 6–22 (2019).
65. Ginn-Hedman, A. M. et al. Diffusible contrast-enhanced micro-CT improves visualization of stented vessels. *Cardiovasc. Pathol.* **60**, 107428 (2022).
66. Vennemann, B., Obrist, D. & Rösgen, T. A smartphone-enabled wireless and batteryless implantable blood flow sensor for remote monitoring of prosthetic heart valve function. *PLoS One* **15**, e0227372 (2020).
67. Jalal, Z. et al. Long-term complications after transcatheter atrial septal defect closure: a review of the medical literature. *Can. J. Cardiol.* **32**, 1315.e11–1315.e18 (2016).
68. Wang, S., Qiao, W. & Dong, N. Residual shunt and microthrombosis associated with new-onset migraine after transcatheter atrial septal defect closure. *Eur. Heart J.* **44**, 4605 (2023).
69. Criscuolo, V. et al. Double-framed thin elastomer devices. *ACS Appl. Mater. Interfaces* **12**, 55255–55261 (2020).
70. Hu, X., Chen, A., Luo, Y., Zhang, C. & Zhang, E. Steerable catheters for minimally invasive surgery: a review and future directions. *Comput. Assist. Surg.* **23**, 21–41 (2018).
71. Safian, R. D. Magnetic navigation: what's the attraction?. *Cathet. Cardiovasc. Interv.* **84**, 668–669 (2014).
72. Limpabandhu, C., Hu, Y., Ren, H., Song, W. & Tse, Z. T. H. Actuation technologies for magnetically guided catheters. *Minim. Invasive Ther. Allied Technol.* **32**, 137–152 (2023).
73. Singh, A. & Mehta, Y. Intraoperative aortic dissection. *Ann. Thorac. Surg.* **18**, 537–542 (2015).
74. Kobayashi, M., Cheng-Kuei, J. & Levesque, D. Flexible ultrasonic transducers. *IEEE Trans. Ultrason. Ferroelectr. Freq. Control* **53**, 1478–1486 (2006).
75. Manwar, R., Kratkiewicz, K. & Avanaki, K. Overview of ultrasound detection technologies for photoacoustic imaging. *Micromachines (Basel)* **11**, 692 (2020).
76. Chen, Y. et al. High-frequency PIN-PMN-PT single crystal ultrasonic transducer for imaging applications. *Appl. Phys. A.* **108**, 987–991 (2012).
77. Schmitz, G. & Dencks, S. Ultrasound imaging. *Recent Results Cancer Res.* **216**, 135–154 (2020).
78. Park, E. Y., Lee, H., Han, S., Kim, C. & Kim, J. Photoacoustic imaging systems based on clinical ultrasound platform. *Exp. Biol. Med. (Maywood.)* **247**, 551–560 (2022).
79. Wang, C. et al. Bioadhesive ultrasound for long-term continuous imaging of diverse organs. *Science* **377**, 517–523 (2022).
80. Lin, M. et al. A fully integrated wearable ultrasound system to monitor deep tissues in moving subjects. *Nat. Biotechnol.* **42**, 448–457 (2024).
81. Liu, T. et al. Flexible thin-film PZT ultrasonic transducers on polyimide substrates. *Sensors* **21**, 1014 (2021).
82. Liu, W., Zhu, C. & Wu, D. Flexible and stretchable ultrasonic transducer array conformed to complex surfaces. *IEEE Electron. Device Lett.* **42**, 240–243 (2021).
83. Zhou, X. et al. Sputtered ZnO film on aluminium foils for flexible ultrasonic transducers. *Ultrasonics* **54**, 1991–1998 (2014).
84. Hu, H. et al. A wearable cardiac ultrasound imager. *Nature* **613**, 667–675 (2023).
85. Yuan, J. et al. Skin-adaptive focused flexible micromachined ultrasound transducers for wearable cardiovascular health monitoring. *Sci. Adv.* **11**, eadw7632 (2025).
86. Kang, D. H. et al. Silicon nanocolumn-based disposable and flexible ultrasound patches. *Nat. Commun.* **16**, 6609 (2025).
87. van Neer, P. L. M. J. et al. Flexible large-area ultrasound arrays for medical applications made using embossed polymer structures. *Nat. Commun.* **15**, 2802 (2024).
88. Ma, J. et al. Procedural simplification in mitral valve transcatheter edge-to-edge repair: full echocardiographic guidance and outcomes. *IJC Heart Vasc.* **59**, 101730 (2025).
89. Dong, J. et al. Embracing a new era of echocardiography-guided percutaneous and non-fluoroscopical procedure for structure heart disease. *Med. Rev.* **5**, 174–176 (2025).

90. Sousonis, V. et al. The use of Intracardiac Echocardiography in Catheter Ablation of Atrial Fibrillation. *Curr. Cardiol. Rep.* **26**, 893–901 (2024).
91. Wang, X., Ji, Z., Yang, S. & Xing, D. Morphological-adaptive photoacoustic tomography with flexible transducer and flexible orientation light. *Opt. Lett.* **42**, 4486–4489 (2017).
92. Huynh, N. T. et al. A fast all-optical 3D photoacoustic scanner for clinical vascular imaging. *Nat. Biomed. Eng.* **9**, 638–655 (2025).
93. Yang, X., Chen, Y. H., Xia, F. & Sawan, M. Photoacoustic imaging for monitoring of stroke diseases: a review. *Photoacoustics* **23**, 100287 (2021).
94. Neprokin, A., Broadway, C., Myllylä, T., Bykov, A. & Meglinski, I. Photoacoustic Imaging in Biomedicine and Life Sciences. *Life (Basel.)* **12**, 588 (2022).
95. Matsumoto, Y. et al. Visualising peripheral arterioles and venules through high-resolution and large-area photoacoustic imaging. *Sci. Rep.* **8**, 14930 (2018).
96. Zhang, Y. et al. Ultrafast longitudinal imaging of haemodynamics via single-shot volumetric photoacoustic tomography with a single-element detector. *Nat. Biomed. Eng.* **8**, 712–725 (2024).
97. Pashaei, V. et al. Flexible body-conformal ultrasound patches for image-guided neuromodulation. *IEEE Trans. Biomed. Circuits Syst.* **14**, 305–318 (2020).
98. de Oliveira et al. Development of a 2.25 MHz flexible array ultrasonic transducer. *Res. Biomed. Eng.* **35**, 27–37 (2019).
99. Shen, S. et al. Effect of aortic arch type on technical indicators in patients undergoing carotid artery stenting. *J. Int. Med. Res.* **47**, 682–688 (2019).
100. Patterson, M. S., Schotten, J., van Mieghem, C., Kiemeneij, F. & Serruys, P. W. Magnetic navigation in percutaneous coronary intervention. *J. Interv. Cardiol.* **19**, 558–565 (2006).
101. Xiong, J., Chen, J. & Lee, P. S. Functional fibers and fabrics for soft robotics, wearables, and human-robot interface. *Adv. Mater.* **33**, e2002640 (2021).
102. Russo, M. et al. Continuum robots: an overview. *Adv. Intell. Syst.* **5**, 2200367 (2023).
103. Khairy, P. Robotic magnetic-guided catheter ablation: an emerging treatment for congenital heart disease. *Future Cardiol.* **21**, 1–3 (2025).
104. Aagaard, P. et al. Remote magnetic navigation: a focus on catheter ablation of ventricular arrhythmias. *J. Cardiovasc. Electrophysiol.* **27**, S38–S44 (2016).
105. Noten, E. lisabeth et al. Robotic navigation shows superior improvement in efficiency for atrial fibrillation ablation. *J. Atr. Fibrillation* **11**, 2108 (2019).
106. Wang, H., Du, J. & Mao, Y. Hydrogel-based continuum soft robots. *Gels* **11**, 254 (2025).
107. Han, W., Gao, W. & Wang, X. Magnetic flexible metastructures: developing smart shape-morphing capabilities at extremely low-temperatures. *Compos. Sci. Technol.* **269**, 111242 (2025).
108. Dreyfus, R. et al. Dexterous helical magnetic robot for improved endovascular access. *Sci. Robot.* **9**, eadh0298 (2024).
109. Srivastava, A., Xu, R., Escoto, A., Ward, C. & Patel, R. V. Design of an ultra thin strain sensor using superelastic nitinol for applications in minimally invasive surgery. *IEEE Int. Conf. Adv. Intell. Mechatron. (AIM)* **2016**, 794–799 (2016).
110. Zhang, M. et al. A magnetically actuated microcatheter with soft rotatable tip for enhanced endovascular access and treatment efficiency. *Sci. Adv.* **11**, eadv1682 (2025).
111. Veeram Reddy, S. R. et al. Invasive cardiovascular magnetic resonance (iCMR) for diagnostic right and left heart catheterization using an MR-conditional guidewire and passive visualization in congenital heart disease. *J. Cardiovasc. Magn. Reson.* **22**, 20 (2020).
112. Knight, D. S. et al. Cardiovascular magnetic resonance-guided right heart catheterization in a conventional CMR environment - predictors of procedure success and duration in pulmonary artery hypertension. *J. Cardiovasc. Magn. Reson.* **21**, 57 (2019).
113. Huang, S. et al. MRI-guided robot intervention—current state-of-the-art and new challenges. *Med-X* **1**, 4 (2023).
114. Tiryaki, M. ehmetE. fe et al. Magnetic guidewire steering at ultrahigh magnetic fields. *Sci. Adv.* **9**, eadg6438 (2023).
115. Williams, S. N., McElhinney, P. & Gunamony, S. Ultra-high field MRI: parallel-transmit arrays and RF pulse design. *Phys. Med. Biol.* **68**, 10 (2023).
116. Haskell, M. W., Nielsen, J. F. & Noll, D. C. Off-resonance artifact correction for MRI: a review. *NMR Biomed.* **36**, e4867 (2023).
117. Li, H. et al. Design and development of novel MRI compatible zirconium- ruthenium alloys with ultralow magnetic susceptibility. *Sci. Rep.* **6**, 24414 (2016).
118. Xue, R. et al. Novel biocompatible Zr-based alloy with low young's modulus and magnetic susceptibility for biomedical implants. *Materials (Basel)* **13**, 5130 (2020).
119. Zhao, X. et al. Permanent fluidic magnets for liquid bioelectronics. *Nat. Mater.* **23**, 703–710 (2024).
120. Li, R. et al. Small-scale magnetic soft robotic catheter for in-situ biomechanical force sensing. *Biosens. Bioelectron.* **270**, 116977 (2025).
121. Fu, S. et al. A magnetically controlled guidewire robot system with steering and propulsion capabilities for vascular interventional surgery. *Adv. Intell. Syst.* **5**, 2300267 (2023).
122. Patel, R. V., Atashzar, S. F. & Tavakoli, M. Haptic feedback and force-based teleoperation in surgical robotics. *Proc. IEEE* **110**, 1012–1027 (2022).
123. Nelson, B. J., Bendok, B. R., Turcotte, E. L. & Batjer, H. H. Remote magnetic navigation enables precision telesurgery. *Sci. Robot.* **9**, eado3187 (2024).
124. Aird, W. C. Endothelial cell heterogeneity and atherosclerosis. *Curr. Atheroscler. Rep.* **8**, 69–75 (2006).
125. Stöger, J. L., Goossens, P. & de Winther, M. P. Macrophage heterogeneity: relevance and functional implications in atherosclerosis. *Curr. Vasc. Pharmacol.* **8**, 233–248 (2010).
126. Yi, Y., Wang, B. & Li, C. Sensors-based monitoring and treatment approaches for in-stent restenosis. *J. Biomed. Mater. Res. B* **111**, 490–498 (2023).
127. van Werkum, J. W. et al. Long-term clinical outcome after a first angiographically confirmed coronary stent thrombosis: an analysis of 431 cases. *Circulation* **119**, 828–834 (2009).
128. Akyildiz, I. F., Su, W., Subramaniam, Y. & Cayirci, E. Wireless sensor networks: a survey. *Comput. Netw.* **38**, 393–422 (2002).
129. Niu, Q. et al. Toward the internet of medical things: architecture, trends and challenges. *Math. Biosci. Eng.* **21**, 650–678 (2024).
130. Selvaraj, N., Nallathambi, G., Moghadam, R. & Aga, A. Fully disposable wireless patch sensor for continuous remote patient monitoring. *Annu. Int. Conf. IEEE Eng. Med. Biol. Soc.* **2018**, 1632–1635 (2018).
131. Abbott, C. A. et al. Innovative intelligent insole system reduces diabetic foot ulcer recurrence at plantar sites: a prospective, randomised, proof-of-concept study. *Lancet Digit. Health* **1**, e308–e318 (2019).
132. Mishra, S., Mohanty, S. & Ramadoss, A. Functionality of flexible pressure sensors in cardiovascular health monitoring: a review. *ACS Sens* **7**, 2495–2520 (2022).
133. Lin, R. et al. Applications of flexible electronics related to cardiocerebral vascular system. *Mater. Today Bio.* **23**, 100787 (2023).
134. Sim, K. et al. An epicardial bioelectronic patch made from soft rubbery materials and capable of spatiotemporal mapping of electrophysiological activity. *Nat. Electron.* **3**, 775–784 (2020).
135. Park, K. et al. 2D material-based injectable sensor for minimally-invasive cerebral blood flow monitoring. *Small* **21**, e2501744 (2025).

136. Chen, J. et al. A noninvasive flexible conformal sensor for accurate real-time monitoring of local cerebral edema based on electromagnetic induction. *PeerJ* **8**, e10079 (2020).
137. Wei, Q. et al. Optimization of LC sensor enabling wireless passive intracranial pressure monitoring. *Microsyst. Technol.* **25**, 3437–3446 (2019).
138. Connor, H. et al. Stretchable, implantable, nanostructured flow-diverter system for quantification of intra-aneurysmal hemodynamics. *ACS Nano* **12**, 8706–8716 (2018).
139. Stauss, M., Htay, H., Kooman, J. P., Lindsay, T. & Woywodt, A. Wearables in nephrology: fanciful gadgetry or Prêt-à-Porter?. *Sensors (Basel)* **23**, 1361 (2023).
140. Zhao, X. et al. Noninvasive diagnosis of early-stage chronic kidney disease and monitoring of the hemodialysis process in clinical practice via exhaled breath analysis using an ultrasensitive flexible NH3 sensor assisted by pattern recognition. *ACS Sens* **10**, 2823–2839 (2025).
141. Matheson, B. T. et al. A novel, microvascular evaluation method and device for early diagnosis of peripheral artery disease and chronic limb-threatening ischemia in individuals with diabetes. *J. Vasc. Surg. Cases Innov. Tech.* **9**, 101101 (2023).
142. Bonetta-Misteli, F. et al. Development and evaluation of a wearable peripheral vascular compensation sensor in a swine model of hemorrhage. *Biomed. Opt. Express* **14**, 5338–5357 (2023).
143. Shabani Varaki, E., Gargiulo, G. D., Penkala, S. & Breen, P. P. Peripheral vascular disease assessment in the lower limb: a review of current and emerging non-invasive diagnostic methods. *Biomed. Eng. Online* **17**, 61 (2018).
144. Ali, S. M. et al. Wearable and flexible sensor devices: recent advances in designs, fabrication methods, and applications. *Sensors (Basel.)* **25**, 1377 (2025).
145. Lim, H. R. et al. Advanced soft materials, sensor integrations, and applications of wearable flexible hybrid electronics in healthcare, energy, and environment. *Adv. Mater.* **32**, e1901924 (2020).
146. Nan, X. et al. Review of flexible wearable sensor devices for biomedical application. *Micromachines* **13**, 1395 (2022).
147. Wang, W. et al. Neuromorphic sensorimotor loop embodied by monolithically integrated, low-voltage, soft e-skin. *Science* **380**, 735–742 (2023).
148. Chen, W. et al. Recent progress in semi-implantable bioelectronics for precision health monitoring. *Adv. Funct. Mater.* **35**, 2424463 (2025).
149. Fang, J. et al. Semi-implantable bioelectronics. *Nano-Micro Lett.* **14**, 125 (2022).
150. Yang, J. et al. Development of smartphone-controlled and microneedle-based wearable continuous glucose monitoring system for home-care diabetes management. *ACS Sens.* **8**, 1241–1251 (2023).
151. Yu, A. et al. Implantable flexible sensors for health monitoring. *Adv. Healthc. Mater.* **13**, e2302460 (2024).
152. Cannata, J. M. et al. Development of a flexible implantable sensor for postoperative monitoring of blood flow. *J. Ultrasound Med.* **31**, 1795–1802 (2012).
153. Gray, M. et al. Implantable biosensors and their contribution to the future of precision medicine. *Vet. J.* **239**, 21–29 (2018).
154. Boutry, C. M. et al. Biodegradable and flexible arterial-pulse sensor for the wireless monitoring of blood flow. *Nat. Biomed. Eng.* **3**, 47–57 (2019).
155. Paula, B. Defining health equity. *J. Nat. Med. Assoc.* **114**, 593–600 (2022).
156. Jabeen, T. et al. An intelligent healthcare system using IoT in wireless sensor network. *Sensors* **23**, 5055 (2023).
157. Osama, M. Internet of medical things and healthcare 4.0: trends, requirements, challenges, and research directions. *Sensors (Basel)* **23**, 7435 (2023).
158. Agarwal, K., Jegadeesan, R., Guo, Y. & Thakor, N. V. Wireless power transfer strategies for implantable bioelectronics. *IEEE Rev. Biomed. Eng.* **10**, 136–161 (2017).
159. Shao, Y. et al. Nanogenerator-based self-powered sensors for data collection. *Beilstein J. Nanotechnol.* **12**, 680–693 (2021).
160. Obuchowicz, R., Strzelecki, M. & Piórkowski, A. Clinical applications of artificial intelligence in medical imaging and image processing-a review. *Cancers* **16**, 1870 (2024).
161. Kulkarni, P. A. & Singh, H. Artificial intelligence in clinical diagnosis: opportunities, challenges, and hype. *JAMA* **330**, 317–318 (2023).
162. Sandeep Ganesh, G., Kolusu, A. S., Prasad, K., Samudrala, P. K. & Nemmani, K. V. S. Advancing health care via artificial intelligence: from concept to clinic. *Eur. J. Pharmacol.* **934**, 175320 (2022).
163. Rezapour et al. Machine learning-enabled prediction of 3D-printed microneedle features. *Biosensors* **12**, 491 (2022).
164. Madika, B. et al. Artificial intelligence for materials discovery, development, and optimization. *ACS Nano* **19**, 27116–27158 (2025).
165. Riesel, A. E. et al. Crystal structure determination from powder diffraction patterns with generative machine learning. *J. Am. Chel. Soc.* **146**, 30340–30348 (2024).
166. Hachem, E. et al. Reinforcement learning for patient-specific optimal stenting of intracranial aneurysms. *Sci. Rep.* **13**, 7147 (2023).
167. Goerzen, D. et al. Machine perception liquid biopsy identifies brain tumours via systemic immune and tumour microenvironment signature. *Nat. Nanotechnol.* Published online December 24, 2025.
168. Ma, L. et al. Liquid biopsy in cancer: current status, challenges and future prospects. *Sig. Transduct. Target Ther.* **9**, 336 (2024).
169. Yang, Z. et al. Magnetic control of a steerable guidewire under ultrasound guidance using mobile electromagnets. *IEEE Rob. Autom. Lett.* **6**, 1280–1287 (2021).
170. Kudithipudi, D. et al. Neuromorphic computing at scale. *Nature* **637**, 801–812 (2025).
171. Xu, M. et al. Reconfigurable neuromorphic computing: materials, devices, and integration. *Adv. Mater.* **35**, e2301063 (2023).
172. Najim, A. et al. An IoT healthcare system with deep learning functionality for patient monitoring. *Int. J. Commun. Syst.* **38**, e6020 (2025).
173. Alharbe, N. & Almalki, M. IoT-enabled healthcare transformation leveraging deep learning for advanced patient monitoring and diagnosis. *Multimed. Tools Appl.* **84**, 21331–21344 (2025).
174. Wang, X. et al. Deep reinforcement learning: a survey. *IEEE Trans. Neural Netw. Learn. Syst.* **35**, 5064–5078 (2024).
175. Liu, M., Shen, X. & Pan, W. Deep reinforcement learning for personalized treatment recommendation. *Stat. Med.* **41**, 4034–4056 (2022).
176. Niraula, D. et al. A clinical decision support system for AI-assisted decision-making in response-adaptive radiotherapy (ARCliDS). *Sci. Rep.* **13**, 5279 (2023).
177. Tseng, H. H. et al. Deep reinforcement learning for automated radiation adaptation in lung cancer. *Med. Phys.* **44**, 6690–6705 (2017).
178. Li, C. et al. Deep reinforcement learning in radiation therapy planning optimization: a comprehensive review. *Phys. Med.* **125**, 104498 (2024).
179. Jiang, L. Y. et al. Health system-scale language models are all-purpose prediction engines. *Nature* **619**, 357–362 (2023).
180. Jarow, J. P. & Baxley, J. H. Medical devices: US medical device regulation. *Urol. Oncol.* **33**, 128–132 (2015).

Acknowledgements

The authors thank Prof. Liping Jiang, Prof. Zehua Qu and Miss Xiaoling Zhu of Fudan University for assistance with knowledge of flexible electronics. The language of this review article has been polished with the assistance of AI-based language tools.

Author contributions

J.G. and L.S. conceptualized the framework and supervised the project. L.Y., Y.Q. and Y.C. wrote the main manuscript text and prepared Figures 1-5 and Table 1. Y.Q. and Y.W. contributed to the literature search and

manuscript revision. Y.C. assisted with the reference collection and formatting. All authors have read and approved the final manuscript.

Competing interests
The authors declare no competing interests.

Additional information
Correspondence and requests for materials should be addressed to Li Shen or Junbo Ge.

Reprints and permissions information is available at http://www.nature.com/reprints

Publisher's note Springer Nature remains neutral with regard to jurisdictional claims in published maps and institutional affiliations.

Open Access This article is licensed under a Creative Commons Attribution 4.0 International License, which permits use, sharing, adaptation, distribution and reproduction in any medium or format, as long as you give appropriate credit to the original author(s) and the source, provide a link to the Creative Commons licence, and indicate if changes were made. The images or other third party material in this article are included in the article's Creative Commons licence, unless indicated otherwise in a credit line to the material. If material is not included in the article's Creative Commons licence and your intended use is not permitted by statutory regulation or exceeds the permitted use, you will need to obtain permission directly from the copyright holder. To view a copy of this licence, visit http://creativecommons.org/licenses/by/4.0/.

© The Author(s) 2026